Supplementary Material

On the Prevalence of Smooth Polymorphs at the Nanoscale: Implications for Pharmaceuticals

Ana M. Belenguer,[1*] Aurora Cruz Cabeza[2,3*], Giulio I. Lampronti,[1,4*] and Jeremy K. M. Sanders[1*]

[1] Department of Chemistry, University of Cambridge, Lensfield Road, Cambridge CB2 1EW, UK

[2] School of Chemical Engineering and Analytical Science, The University of Manchester, Oxford Road, Manchester, UK, M13 9PL, UK.

[3] Astra Zeneca, Silk Road Business Park, Charter Way, Macclesfield, SK10 2NA, United Kingdom

[4]Department of Earth Sciences, University of Cambridge, Downing Street, Cambridge CB2 3EQ, UK

Corresponding authors: amb84@cam.ac.uk, JKMS@cam.ac.uk, gil21@cam.ac.uk, aurora.cruzcabeza@manchester.ac.uk

KEYWORDS: mechanochemistry; milling; nanocrystals; Scherer size; Rietveld and Pawley refinements

INDEX

Nomenclature and abbreviations used

LAG	Refers to ball mill liquid assisted grinding. The term “LAG” is equivalent and assumes we are discussing ball mill LAG
NG	Refers to ball mill neat grinding. The term “NG” is equivalent and assumes we are discussing ball mill neat grinding
CAF	Caffeine [58-08-2]
D-sorb	D-sorbitol [50-70-4]
CPA	Chlorpropamide [94-20-2]
APAA	N-acetyl-1-phenylalanine amide [7376-90-1]
MeCN	Acetonitrile
H_2O	water
PXRD	Powder X-ray diffractometry
ID	Internal diameter
Hz	Hertz (frequency used to swing the grinding jars by the ball mill grinder)
ss	Stainless steel

1 Experimental Section: Materials and Equipment

1.1 Chemicals and Materials

All solvents used for ball mill grinding experiments were obtained as follows: acetonitrile (MeCN, were laboratory reagent grade, ≥99.8% from Fisher). The drying agent used in the desiccator is Drierite, a calcium sulfate with indicator (blue=dry; pink=wet), 8 mesh [7646-79-9] from Acros Organics.

Anhydrous Caffeine [58-08-2] from Sigma Aldrich; D-sorbitol [50-70-4] Across Organics, 97%; Chlorpropamide (1-(4-Chlorophenylsulfonyl)-3-propylurea), from TCI, >99.0% (Transmission)and N-acetyl-1-phenylalanine amide [7376-90-1], must be stored at 2-8^{o}C, from BACHEM, >99%(TLC).

The screw closure jars were machined in house from AISI440C stainless steel. The hardening and tempering process of the AISI440C stainless steel screw closure jars to achieve a hardening of + 56HRC was performed by WALLWORK CAMBRIDGE LTD. The 7 mm diameter 440C stainless steel ball bearings were obtained from Dejay Distribution Ltd in UK. PXRD sample glass slides were manufactured in house.

1.2 Equipment

1.2.1 Ball mill grinder

The ball mill grinding experiments were all performed using in a Retsch MM400 Shaker Mill with the safety cover removed as the grinder motor vents to the front of the equipment warming the grinding jars on prolonged grinding. An external safety shield was used for safety.

a) b)

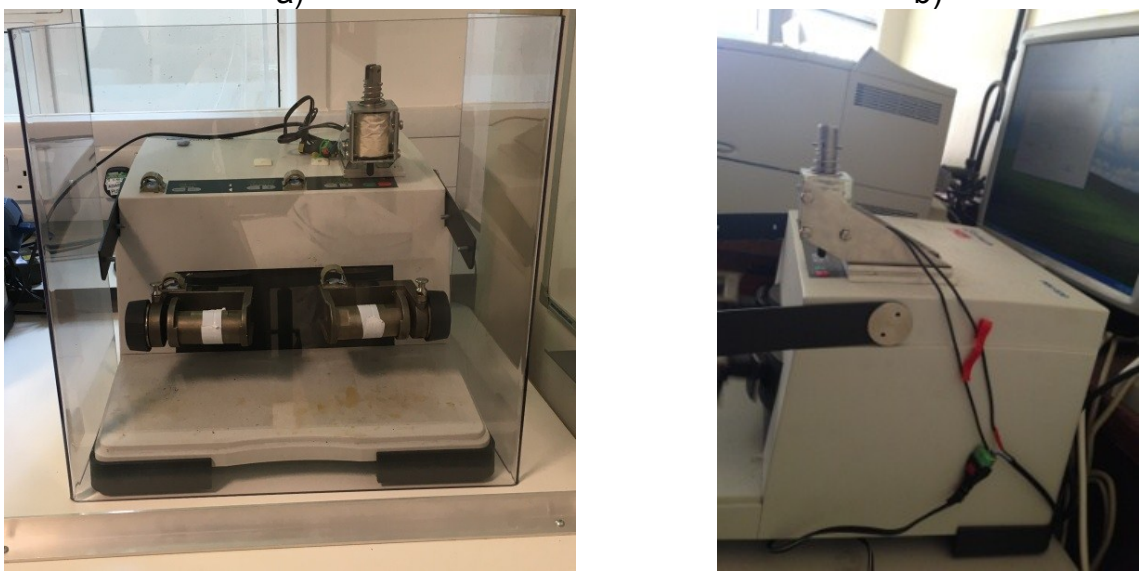

Figure S 1 Modified Retsch MM400 Shaker Mill (ball mill grinder) a) seen from the front with the built-in safety cover from Retsch removed and replaced by an external safety shield. 2 screw closure jars are fitted as used for the solvent equilibration curve experiments described here. The homemade solenoid used as a push button is installed over the START button to automatically start the grinding and b) side view of the push button.

1.2.2 Automated solenoid to press the Retsch MM400 Shaker Mill start button

Retsch MM400 Shaker Mill stops automatically once the run time has elapsed. It can only be automatically run for a maximum of 99 minutes. As these studies required in many cases up to multi hours grinding, an automated solenoid was manufactured in-house and controlled with in-house software to press repeatedly the START button as often as the experiment required it. (See Figure S 1b). The software allows the start of grinding to be scheduled so as to finish the grinding experiment when desired. To prevent the Retsch MM400 motor from overheating, 5-10 minutes rest was allowed for each hour grinding.

1.3 Grinding jars

1.3.1 Screw closure grinding jars with Teflon washer

The grinding jars were manufactured in-house from AISI440C stainless steel with the same internal dimensions and volume (14.5 mL internal volume: 19 mm ID x 54mm internal length) as the snap closure grinding jars prepared from 316 Stainless steel used in previous publications [1, 2] the closure being a screw closure lined with a Teflon washer to ensure good sealing when the grinding jar is closed. 316 Stainless steel is relatively soft tested as -5 HRC (HRC stands for Rockwell Hardness measured on the C scale) and the thread is easily damaged on extensive grinding and requires continuous maintenance. To avoid this damage, screw closure jars were machined in-house from AISI440C stainless steel and the cleaned machined jars were subjected to a hardening and tempering process to reach + 56HRC. This design should prevent the escape of the vapor phase of the solvent and also prevent powder and added solvent from being trapped in the junction of the closure while avoiding damage to the thread of the screw closure. These grinding jars were used for polymorph interconversion turnover experiments.

Figure S 2 14.5mL Stainless steel screw closure grinding jars with Teflon washer.

1.4 Balance

A Mettler Toledo XPE 205 Delta Range with an accuracy of 0.01mg was used for weighing the starting materials using weighing paper.

1.5 Automatic pipettes

A Sartorius eLINE Picus Electronic Pipette, 1-channel, 5 - 120 μL, in combination with Sartorius SafetySpaceTM, Low Retention, 2-120 μL, Sterile Filter Tip was used to achieve maximum accuracy allowing an accurate increment of 0.1 μL to be pipetted. The systematic error disclosed by the manufacturers in the pipette specification is: for 120μL is ±0.48 μL, for 60 μL is ±0.36 μL and for 12 μL is ±0.24 μL.

The Picus pipette was primed repeatedly for each solvent until the liquid was securely held by the pipette tip before dispensing the selected volume of the solvent. All solvent except DCM were pipetted with direct pipetting technique: the full volume of the solvent aspirated by the automatic pipette, was automatically dispensed to the grinding jar; no residual solvent remained in the pipette tip.

1.6 PXRD equipment

X-ray powder diffractograms in the 2θ range 5-45° (Cu Kα radiation, step size 0.03°, time/step 100 s, 0.04 rad soller, VxA 40x40 with a total time of 13 minutes) were collected on a Panalytical X'Pert Pro diffractometer equipped with an X'Celerator detector operating in reflection geometry. The PXRD sample slide was mounted on the slide bracket The PXRD equipment was available at the Department of Chemistry, University of Cambridge.

1.6.1 PXRD glass slides

Glass PXRD sample slide (10x15 mm) with the 2 mm rectangular recess

2 Experimental Section: methodology

2.1 Procedure for the interconversion between LAG-polymorph and NG polymorph an vice versa for the four systems under study

2.1.1 Experimental strategy and considerations

For all the four systems discussed here, we started from 300 mg of the commercially available material as powder is continuously being lost on transferring it to and from the grinding jar to the PXRD sample slide immediately after the termination of each turnover grinding experiment. Additionally, many of these systems when run under long NG conditions resulted in the formation of very static powder which was very difficult to transfer to a PXRD sample slide even with the use of deionizing guns and further contributed to the loss of powder for the turnover experiments.

For all the four systems studied, the commercially available material is the bulk stable polymorph and these PXRD traces are consistent with the LAG-polymorph obtained by LAG.

To ensure that the solvent did not escape during grinding from the junction in the screw closure grinding jar, the jars were well secured by wrapping the junction tightly with insulating tape. In all cases, we have removed the front cover from the MM400 and substituted it with an external safety screen to avoid the venting of the grinding motor of the MM400 heating the space where the grinding jars are moving (See Section 1.2.1). Thermodynamic equilibrium can change with the increase of temperature of the grinding reaction. To avoid the jar from heating up due to extensive continuous grinding (See Section 1.2.2 for automation of grinding), the grinder was stopped for 5 minutes for every hour grinding at 30 Hz to allow the motor to rest and the jars to cool down to ambient temperature.

NG starting from the commercially available material (LAG-polymorph) did not present any problem and resulted, given enough grinding time, in the quantitative formation of the NG-polymorph. However, when starting from the *in-situ* formed LAG-polymorphs obtained by LAG, the success or failure of the formation of the quantitative NG-polymorph depended on how successfully the residual solvent could be removed from the LAG-polymorph. Leaving the *in-situ* LAG-polymorph drying in the fumehood was enough for all studied cases except for D-sor. . However we learned that having a container with water in the fumehood would result in the-*situ* dried LAG-polymorph adsorbing moisture, this preventing the transformation to the NG-polymorph even with extensive NG. Efficient drying of the wet powder can be achieved, when needed, by allowing the open jars to dry in a desiccator containing dry Drierite desiccant.

The LAG-polymorph can be converted to the NG-polymorph by NG. NG often leads to very broad signals suggesting that they contain amorphous form.[3] Extensive NG improves the crystallinity of the NG-polymorph.[3] The use of alkyl solvents by LAG, such as n-heptane can lead to the same NG-polymorph as by NG but much more crystalline. Use of LAG with polar solvents, like acetonitrile or water, transforms the NG-polymorph form to the LAG-polymorph.

Two 7mm ball bearing have been used for this payload as done previously for the $2NO_2PhSSPh4Cl$ project.[2, 4, 5] We have published the careful methodology we use for ball mill grinding experiments in a video article in JoVe (Journal of visualised Experiments).[4]

An example of one polymorph interconversion turnover experiment is as follows: first, the conversion of the commercially available material (LAG-polymorph) to NG-polymorph by NG; this NG-polymorph is then converted back to the LAG-polymorph by LAG adding the required type and concentration of the solvent. For a second turnover experiment, this procedure is repeated again.

2.1.2 Caffeine anhydrous: procedure for turnover experiments

Caffeine anhydrous [58-08-2] is commercially available as the stable-bulk polymorph (form II, CCDC code NIWFEE02). For the metastable bulk polymorph obtained by ball mill NG, the PXRD is inconsistent with the polymorph reported in the literature or alternatively the structural model documented in the CCDC database is wrong. We therefore will code it as form III. Method development is discussed in Section 3.1, while polymorph interconversion turnover experiments are discussed in Section 4.1.

2.1.2.1 Conversion from LAG-polymorph to NG-polymorph for CAF

300 mg of caffeine anhydrous commercially available starting material (form II) was transferred to a screw closure jar. Two 7mm diameter 440C ss ball bearings were added. Nothing else was added for NG. The jar was closed and secured with tape. 45 minutes NG at 30Hz sufficed to convert form II to the metastable-bulk polymorph form III.

The same procedure could be applied to form II, obtained *in-situ* by polymorph conversion from form III by LAG as explained in the next Section 2.1.2.2. It was important to ensure that the residual solvent remaining in the sample of form II was allowed to dry either in the fumehood or in the desiccator containing dry Drierite before performing a new NG experiment.

2.1.2.2 Conversion from NG-polymorph to LAG-polymorph for CAF

50μL of MeCN was added to the jar containing *in-situ* form III obtained by NG from the commercially available materials as described in the previous Section 2.1.2.1. The jar was closed and secured with tape. 15 min LAG at 30Hz sufficed to convert it back to Form II.

2.1.3 D-sorbitol: procedure for turnover experiments

D-sorbitol [50-70-4] is commercially available as the stable-bulk polymorph form γ (CCDC code GLUCIT03). The NG- polymorph is form α (CCDC code GLUCIT01). Method development is discussed in Section 3.2, while polymorph interconversion turnover experiments are discussed in Section 4.2.

2.1.3.1 Conversion from LAG-polymorph to NG-polymorph for D-Sor

300 mg of D-sorbitol commercially available material (form γ) was transferred to a screw closure jar. Two 7mm diameter 440C ss ball bearings were added. Nothing else was added for the NG experiment. The jar was closed and secured with tape. 8h NG at 30Hz sufficed to convert form γ to NG polymorph form α in a crystalline form. However 2h NG was shown also to be sufficient to obtain form α quantitatively, though the Braggs peaks were broader suggesting it contained amorphous material.[3]

The same procedure could be applied to the LAG-polymorph form γ obtained *in-situ* by polymorph conversion from the NG-polymorph form α by LAG as explained in the next Section 2.1.3.2. It was important to ensure that the residual solvent remaining in the LAG sample was allowed to dry in the desiccator containing dry Drierite before performing a new NG experiment.

2.1.3.2 Conversion from NG-polymorph to LAG-polymorph for D-Sor

50μL of MeCN was added to the jar containing in-situ NG polymorph form α obtained by NG the commercially available materials form γ (LAG polymorph) as described in the previous Section 2.1.3.1. The jar was closed and secured with tape. 1h LAG at 30Hz sufficed to convert the NG- polymorph form α back to the LAG polymorph form γ.

2.1.4 Chlorpropamide: procedure for turnover experiments

Chlorpropamide [94-20-2] is commercially available as the stable-bulk polymorph form β. The metastable bulk polymorph is form η. Method development is discussed in Section 3.3, while polymorph interconversion turnover experiments are discussed in Section 4.3.

2.1.4.1 Conversion from LAG-polymorph to NG-polymorph for CPA

300 mg of chlorpropamide commercially available starting material (form β) was transferred to a screw closure jar. Two 7mm diameter 440C ss ball bearings were added. Nothing else was added for the NG experiment. The jar was closed and secured with tape. 6 h NG at 30Hz was used to convert form β to form η. 6hour grinding may have been in well in excess of what was needed for the transformation.

The same procedure could be applied to the stable-bulk form β obtained *in-situ* from form η by LAG as explained in the next Section 2.1.4.2. It was important to ensure that the residual solvent remaining in the LAG sample was allowed to dry either in the fumehood or in the desiccator containing dry Drierite before performing a new NG experiment.

2.1.4.2 Conversion from NG-polymorph to LAG-polymorph for CPA

50μL MeCN was added to the jar containing in-situ form η obtained by NG the starting materials as described in the previous Section 2.1.4.1, and the jar closed and secured with tape. 1h LAG at 30Hz sufficed to convert form η back to the stable-bulk form β.

2.1.5 N-acetyl-1-phenylalanine amide: procedure for turnover experiments

N-acetyl-1-phenylalanine amide [7376-90-1] is commercially available as the stable-bulk polymorph form γ. The metastable bulk polymorph is form α. The structural model for form γ and form α discussed by Altheimer et al[6] have not been deposited in the CCDC database. . Method development is discussed in Section 3.4, while polymorph interconversion turnover experiments are discussed in Section 4.4.

2.1.5.1 Conversion from LAG-polymorph to NG-polymorph for apaa

300 mg of N-acetyl-1-phenylalanine amide commercially available starting material (form γ) was transferred to a screw closure jar. Two 7mm diameter 440C ss ball bearings were added. Nothing else was added for NG. The jar was closed and secured with tape. 45 min NG at 30Hz sufficed to convert it to the metastable-bulk form α.

The same procedure could be applied to stable-bulk form γ obtained *in-situ* by polymorph conversion from metastable-bulk form α by LAG as explained in next Section 2.1.5.2. It was important to ensure that the residual solvent remaining in the LAG sample was allowed to dry either in the fumehood or in the desiccator containing dry Drierite before performing a new NG experiment.

2.1.5.2 Conversion from NG-polymorph to LAG-polymorph for apaa

50μL MeCN was added to the jar containing *in-situ* metastable-bulk form α obtained by NG from the starting materials as described in previous Section 2.1.5.1, and the jar was closed and secured with tape. 1h LAG at 30Hz sufficed to convert form α back to the stable-bulk form γ.

2.2 PXRD data analysis

2.2.1 Indexing of NG-polymorph of caf

The data for form III were analysed using the software DASH v3.3.6.2. Fourteen peaks were chosen and their position determined in the 2θ range 5 to 40º. An orthorhombic unit cell was found using the algorithm DICVOL1 with a volume of 1956 Å3 (a = 18.298 Å, b = 12.874 Å, c = 8.312 Å). The volume is consistent with eight molecules of caffeine (Z=8). Space group statistics suggested sp. gr. P212112, corresponding to Z' = 2.

2.2.2 *Indexing of NG-polymorph of cpa*

The data for form η were analysed using the software DASH v3.3.6. Twenty peaks were chosen and their position determined in the 2θ range 5 to 22º. A monoclinic unit cell was found using the algorithm DICVOL with a volume of 2664 Å3 (a = 14.533 Å, b = 16.231 Å, c = 11.378 Å, β = 96.92). The volume is consistent with eight molecules of chlorpropamide (Z=8). Space group statistics suggested sp. gr. P21/n, corresponding to Z' = 2.

2.2.3 *Rietveld and Pawley refinements*

Rietveld and Pawley refinements were performed with the software Topas V6.[7] Details about the refinements setup are given in the SI. The known crystal structures for caf, cpa and d-sor polymorphs were retrieved from the CCDC.[8] The crystal structure for the apaa NG- and LAG-polymorphs were retrieved from Altheimer et al. 2009. [6] No structural parameter other than the unit cell parameters was refined in the Rietveld refinements. Furthermore the peak shape and the parameters describing the diffractometer geometry were optimized using the LaB_6 660b NIST standard: only a Lorentzian Scherrer term (CS_L) for each phase was modeled in the Pseudo-Voigt functions for the quantitative analysis, the other parameters being fixed. A shifted Chebyshev function with seven parameters was used to fit the background. Spherical harmonics were used to model preferred orientation

2.2.3.1 *Rietveld and Pawley refinements for caf*

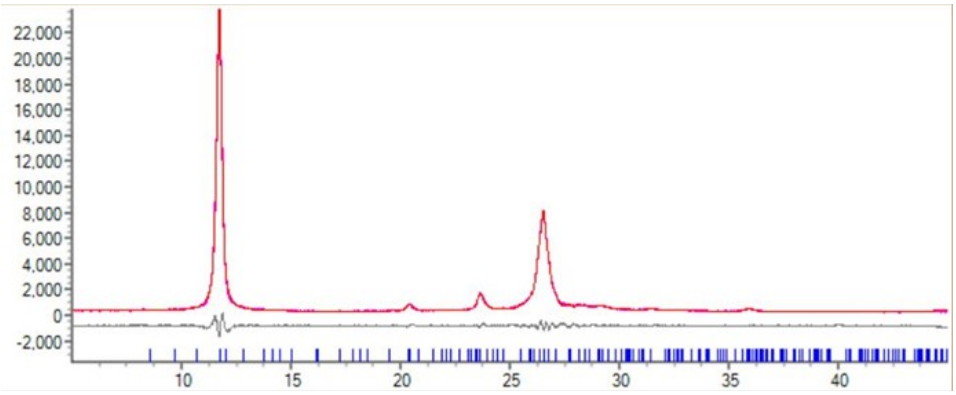

Figure S 3 Plot of observed (purple), calculated (red) and difference (grey) curves from one of the Pawley refinements for the NG- polymorph (form III) of caf (blue marks). The x-axis is in degrees of 2θ the y-axis is in counts. The χ2 and Rwp at convergence were equal to 2.14 and 7.55 respectively.

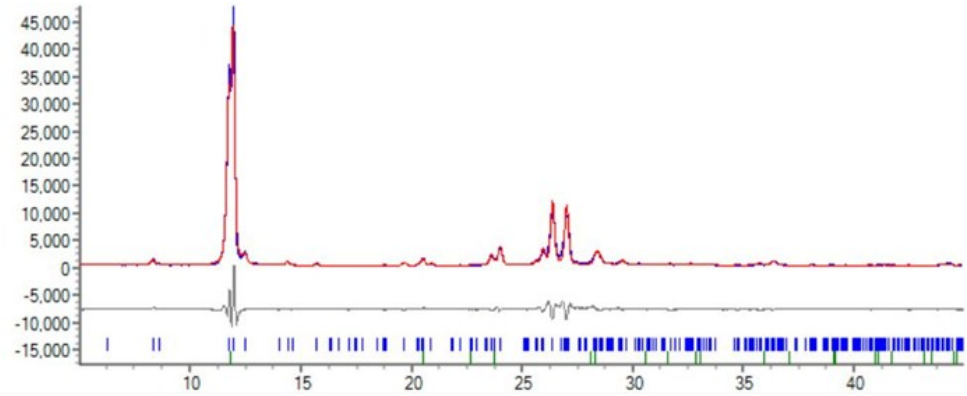

Figure S 4 Plot of observed (blue), calculated (red) and difference (grey) curves from one of the Pawley refinements for the LAG-polymorph (form II) of caf (Form II, blue marks). The x-axis is in degrees of 2θ the y-axis is in counts. The χ2 and Rwp at convergence were equal to 4.74 and 13.75 respectively

2.2.3.2 Rietveld and Pawley refinements for cpa

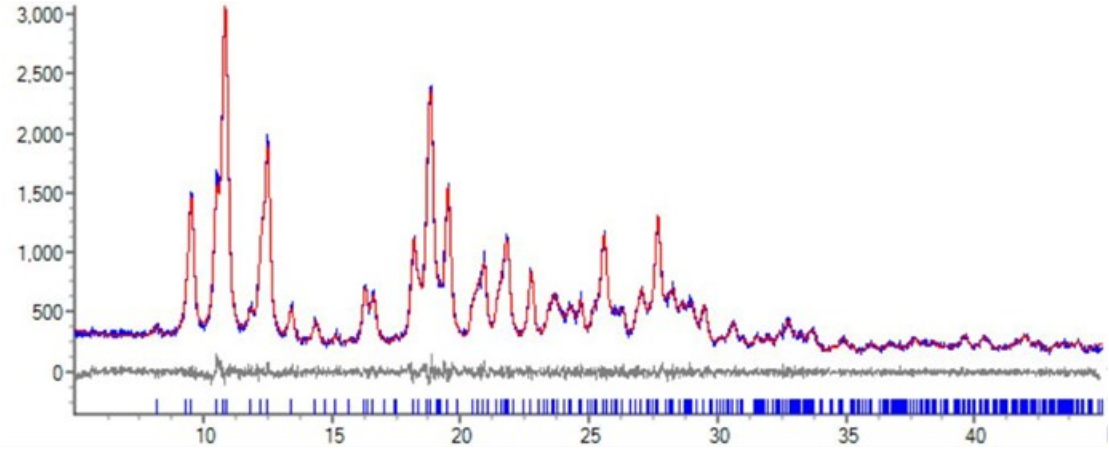

Figure S 5 Plot of observed (purple), calculated (red) and difference (grey) curves from one of the Pawley refinements for the NG-polymorph (form η) of cpa (blue marks). The x-axis is in degrees of 2θ the y-axis is in counts. The χ2 and Rwp at convergence were equal to 1.23 and 5.37 respectively

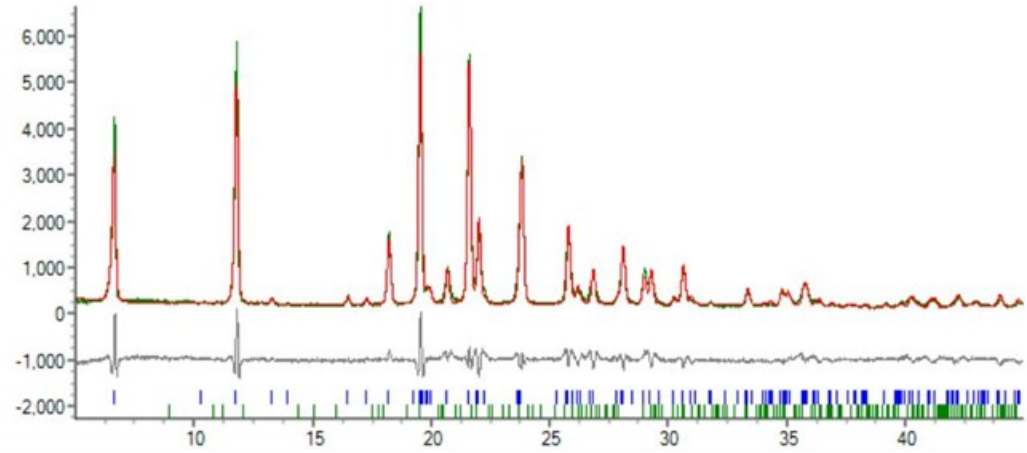

Figure S 6 Plot of observed (purple), calculated (red) and difference (grey) curves from one of the Rietveld refinements for the LAG-polymorph of cpa (form β), blue marks). The x-axis is in degrees of 2θ the y-axis is in counts. The χ2 and Rwp at convergence were equal to 2.88 and 14.40 respectively.

2.2.3.3 Rietveld and Pawley refinements for D-sor

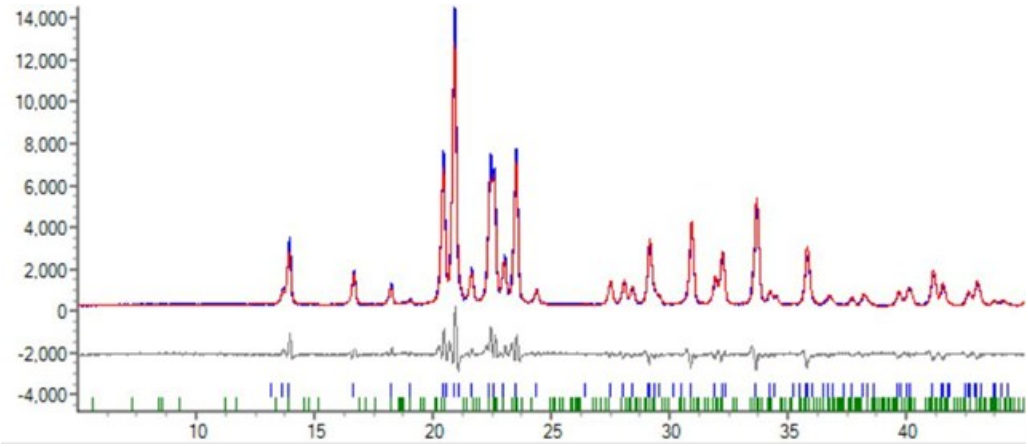

Figure S 7 Plot of observed (blue), calculated (red) and difference (grey) curves from one of the Rietveld refinements for the NG-polymorph of d-sor (form α, blue marks). The x-axis is in degrees of 2θ the y-axis is in counts. The $\chi 2$ and Rwp at convergence were equal to 3.19 and 11.42 respectively.

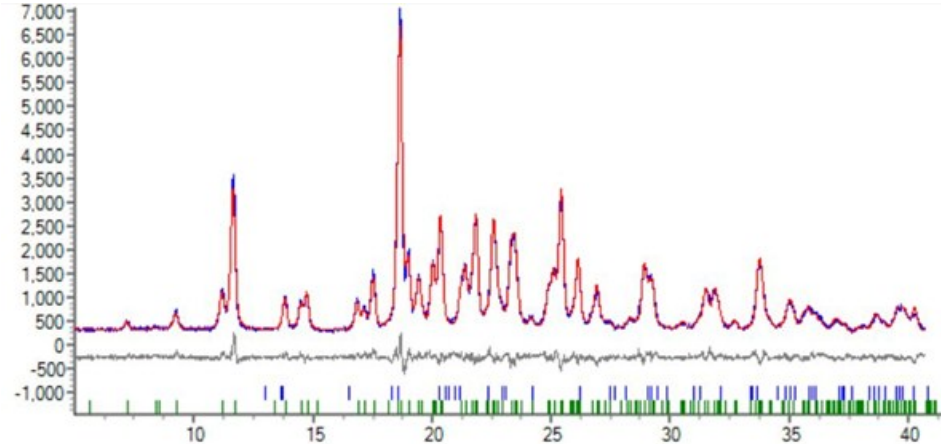

Figure S 8 Plot of observed (blue), calculated (red) and difference (grey) curves from one of the Rietveld refinements for the LAG-polymorph of d-sor (form γ, green marks). The x-axis is in degrees of 2θ the y-axis is in counts. The $\chi 2$ and Rwp at convergence were equal to 1.74 and 6.37 respectively.

2.2.3.4 *Rietveld and Pawley refinements for apaa*

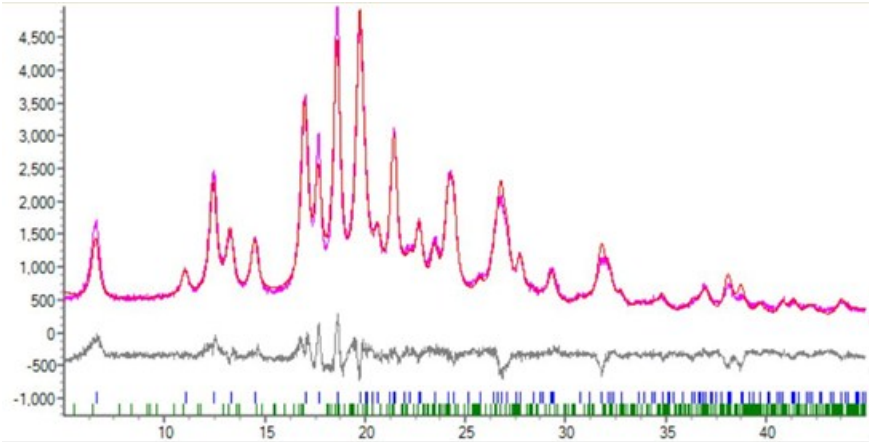

Figure S 9 Plot of observed (purple), calculated (red) and difference (grey) curves from one of the Rietveld refinements for the NG-polymorph of apaa (form α, blue marks). The x-axis is in degrees of 2θ the y-axis is in counts. The χ2 and Rwp at convergence were equal to 2.42 and 7.73 respectively.

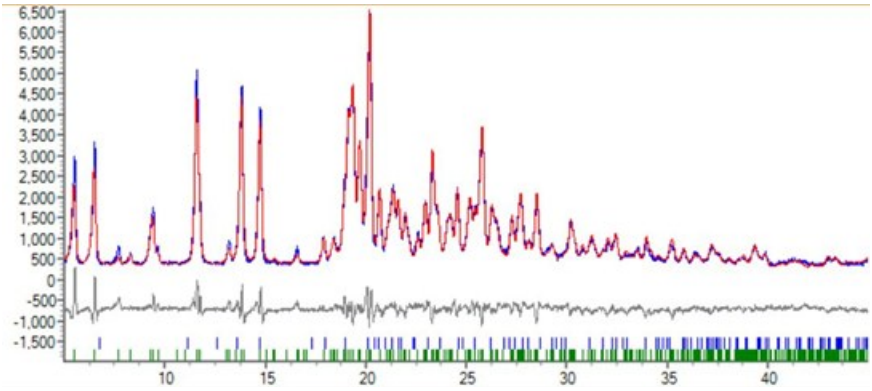

Figure S 10 Plot of observed (blue), calculated (red) and difference (grey) curves from one of the Rietveld refinements for the LAG-polymorph of apaa (form γ, green marks). The x-axis is in degrees of 2θ the y-axis is in counts. The χ2 and Rwp at convergence were equal to 2.81 and 9.25 respectively.

2.2.4 *Sample preparation for PXRD analysis*

On completion of the grinding experiment, the grinding jar was immediately opened, the powder transferred to grease –proof weighing paper and gently ground with a spatula taking care not to lose any powder. Static powder was allowed to rest on an ionizer to improve the transferability of the powder. The powder was transferred to the sample holder (See Section 1.6.1) for Powder X-Ray diffractometry.

2.3 Crystal size determination from powder diffraction data

Because of the nanocrystalline nature of the analysed powders and the absence of peaks above 45º in 2θ, the sample contribution to the peak broadening was assumed to be related to size only. A Lorentzian peak shape was found to fit better than a Gaussian one. In order to minimise the correlations and the e.s.d., the crystal size contribution to peak broadening was modelled as isotropic, i.e. using one single parameter for all crystallographic directions. We here remind that the e.s.d. from the Rietveld calculation has no bearing on the precision or accuracy, being merely related to the mathematical fit of the model. For what concerns the accuracy of the size determination, it is known that for a typical laboratory X-ray diffraction instrument the Scherrer analysis provides sensitivity to crystallite size in the 1–100 nm range, the upper limit being set by the instrumental broadening. This also means that the smaller the crystal size, the less the Scherrer size value is affected by how the instrumental broadening is defined.[9] In our experience, a Scherrer crystal size of 100nm can vary by up to 30% relative of its value depending on the way the fundamental parameters are used to fit the LaB6 standard - e.g., depending on whether the size and microstrain contribution for the standard are assumed to be zero or are allowed to give a contribution to the peak shape. However, if the crystal size is 60nm, this variation is no more than 10% relative. In other words, the smaller the crystal size, the more reliable the estimate is. It is also important to point out that the peak shape tends to be dominated by the larger crystallites rather than the smaller ones, so the calculated size tends to be overestimated.[9]

3 Experimental Section: Method development for polymorph interconversion

3.1 Method development for Caffeine anhydrous

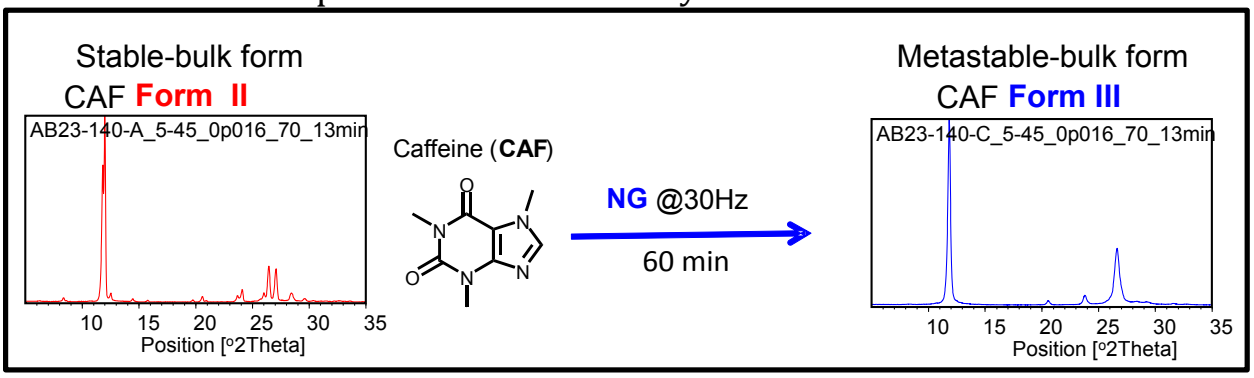

Figure S 11 Chemical structure of Caffeine, PXRD of the stable-bulk polymorph form II corresponding to commercially available compound and PXRD of metastable-bulk polymorph form III obtained by NG from form II.

The polymorph transformation of the stable-bulk form II (β) (here named form II) to the metastable-bulk Form I (α) (here named form III) for Caffeine anhydrous by NG had been reported by Boldyreva's group[10] and Hédoux et al[11].

NG of the commercially available stable-bulk form II of Caffeine anhydrous as described in Section 2.1.2.1 resulted in the quantitative formation of form III within 45 min at 30Hz. The quantitative transformation of form III back again into form II could be achieved within 15 min LAG (50μL MeCN) at 30Hz. The milling time and volume of solvent were arbitrarily selected to achieve thermodynamic control. No further method development was required for this system and all the data is reported in the polymorph interconversion turnover experiments as described in Section 3.1.

3.2 Method development for D-sorbitol

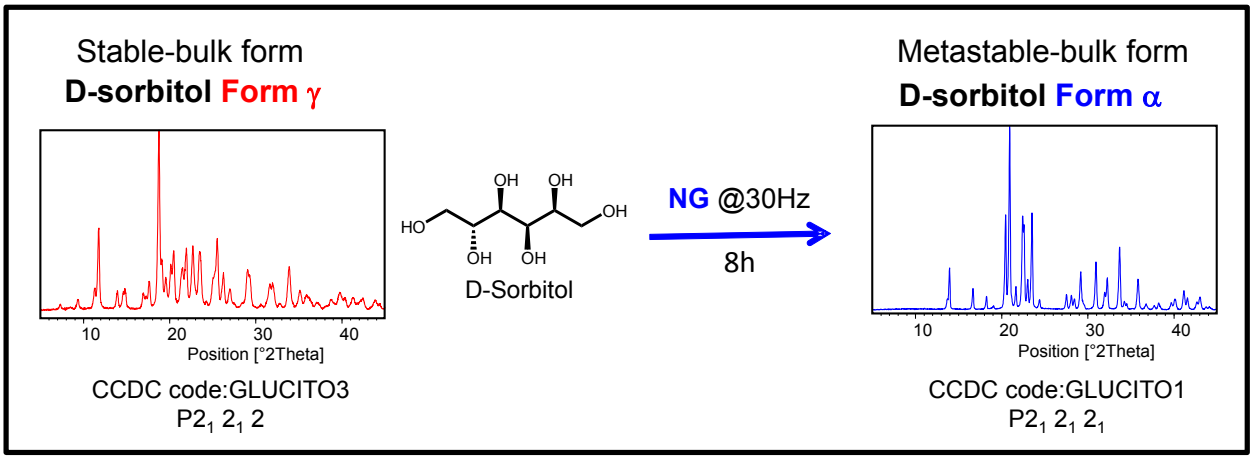

Figure S 12 Chemical structure of D-Sorbitol, PXRD of the stable-bulk polymorph form γ corresponding to commercially available compound and PXRD of metastable-bulk polymorph form α obtained by NG of form γ. CCDC codes for form γ and form α polymorphs of D-Sorbitol.

The polymorph transformation of the stable-bulk Form γ (here also named form γ) by NG to the NG-polymorph Form α (here also named form α) for D-sorbitol had been reported by Descamps group.[3] This paper has a in depth study of the stages which the D-sorbitol adopts from micrometer size crystal (commercially available product) form γ to the NG-polymorph form α by NG going via amorphosized steps. Extensive NG grinding (10 h) was shown to improve the crystallinity and reduced the broadening of the Braggs peaks as compared to 2h milling.[3]

We therefore adopted 8 hours for NG starting with the of the commercially available compounds form γ (fig. S13-a), forming the NG-polymorph (form α) with good Bragg peaks (fig. S13-b). The addition of 50μL of MeCN to form α and 1h LAG at 30 Hz resulted in the quantitative transformation to form γ (fig. S13-c). The jar was initially opened and left in the fumehood to dry overnight; this was found not to be successful (fig. S13-d), even when left in the fumehood over a few days (fig. S13-e) as indicated by the fact that the sample of form γ was no longer being transformed to the NG-polymorph (form α) even after extensive NG at 30 Hz. The open jar was then transferred to a desiccator over dry Drierite and left to dry overnight. The jars were then closed and NG for 8h at 30 Hz finally resulting in quantitative transformation to the NG-polymorph form α (fig. S13-f). This proves that it is very important to totally remove the solvent before doing NG for some systems. The extended milling time and volume of solvent were arbitrarily selected to achieve thermodynamic control and improved crystallinity.

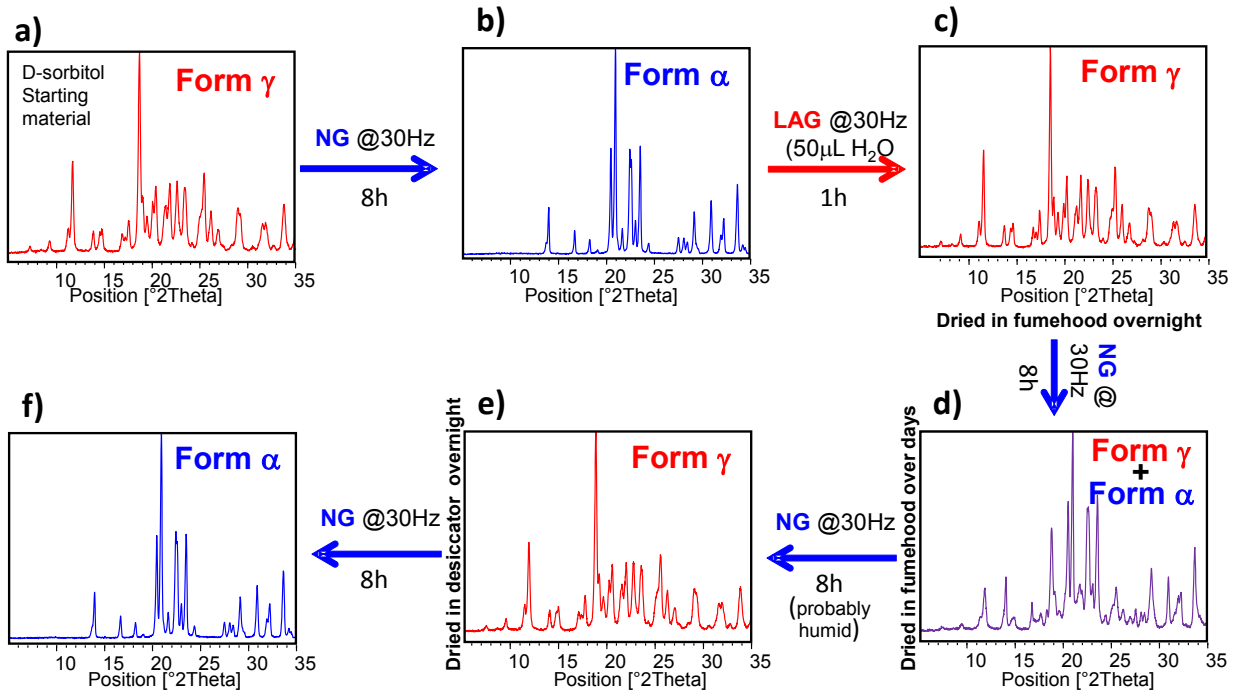

Figure S 13 Method development for D-sor a) starting from commercially available product (form γ); after that showing the PXRD of the resulting powder on completion of grinding; b) transformation to form α by NG; c) transformation of form α to form γ by LAG with water; d) poor drying in fumehood of form γ results on NG only to partial transformation to form α, e) the transformation of the mixture of form α & form γ to quantitative form γ can only be explained by the sample becoming humid in the fumehood which had a sonicator with water; f) drying the sample in a dessicator over dried Drierite and further NG results in the transformation to quantitative form α.

3.3 Method development for Chlorpropamide

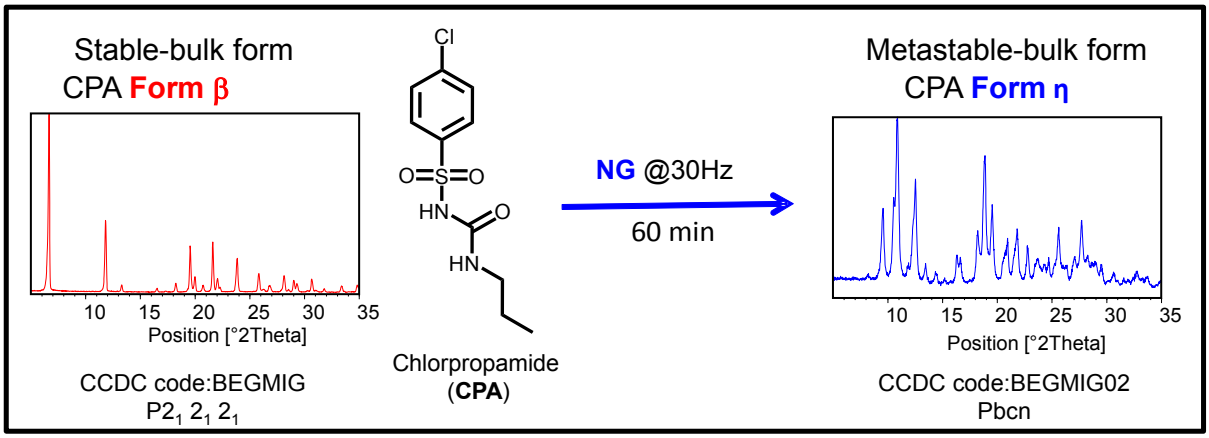

Figure S 14 Chemical structure of chlorpropamide, PXRD of the stable-bulk polymorph Form β corresponding to commercially available compound and PXRD of metastable-bulk polymorph Form η obtained by NG of Form β..

Several polymorphs of chlorpropamide have been reported, Form ε (here named Form β) being the stable-bulk form.[12] The partial polymorph transformation due to limited milling time of the stable-bulk Form ε to the metastable-bulk Form β (here named as Form η) for chlorpropamide under NG (dry environment) and that of the metastable-bulk Form β and Form α to the stable-bulk Form ε in a humid atmosphere had been reported by Boldyreva's group.[13]

NG of the commercially available stable-bulk Form β of chlorpropamide resulted in the quantitative transformation into a new unreported metastable-bulk Form η within 6h at 30Hz. The quantitative transformation of the Form η back again into Form β could be achieved within 1h LAG (50μL MeCN) at 30Hz. The milling time and volume of solvent were arbitrarily selected to achieve thermodynamic control and in the case of NG to obtain a crystalline material. No further method development was required for this system and all the data is reported in the polymorph interconversion turnover experiments described in Section 4.3.

3.4 Method development for for N-Acetyl-L-phenylalanine amide

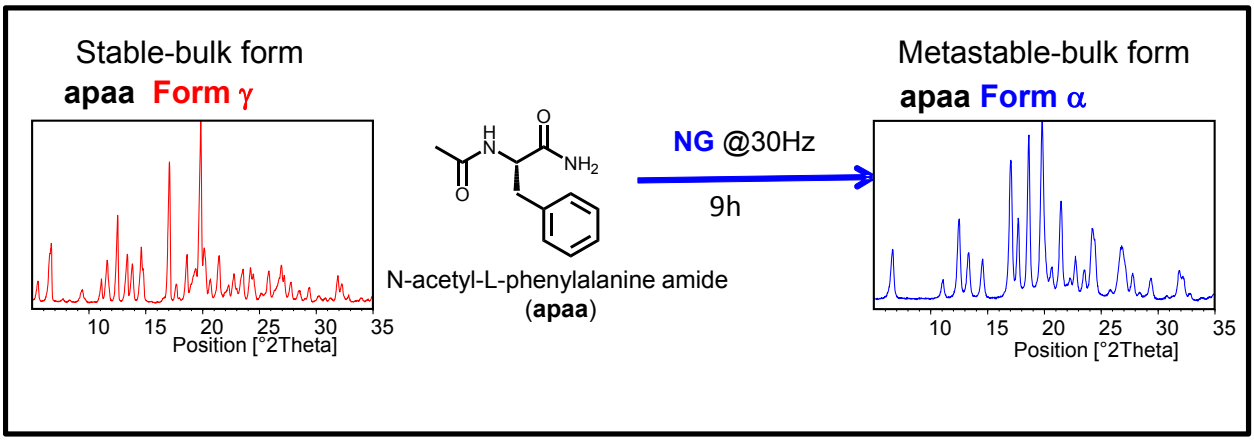

Figure S 15 Chemical structure of N-acetyl-L-phenylalanine amide, PXRD of the stable-bulk polymorph Form γ corresponding to commercially available compound and PXRD of metastable-bulk polymorph Form α obtained by NG of Form γ.

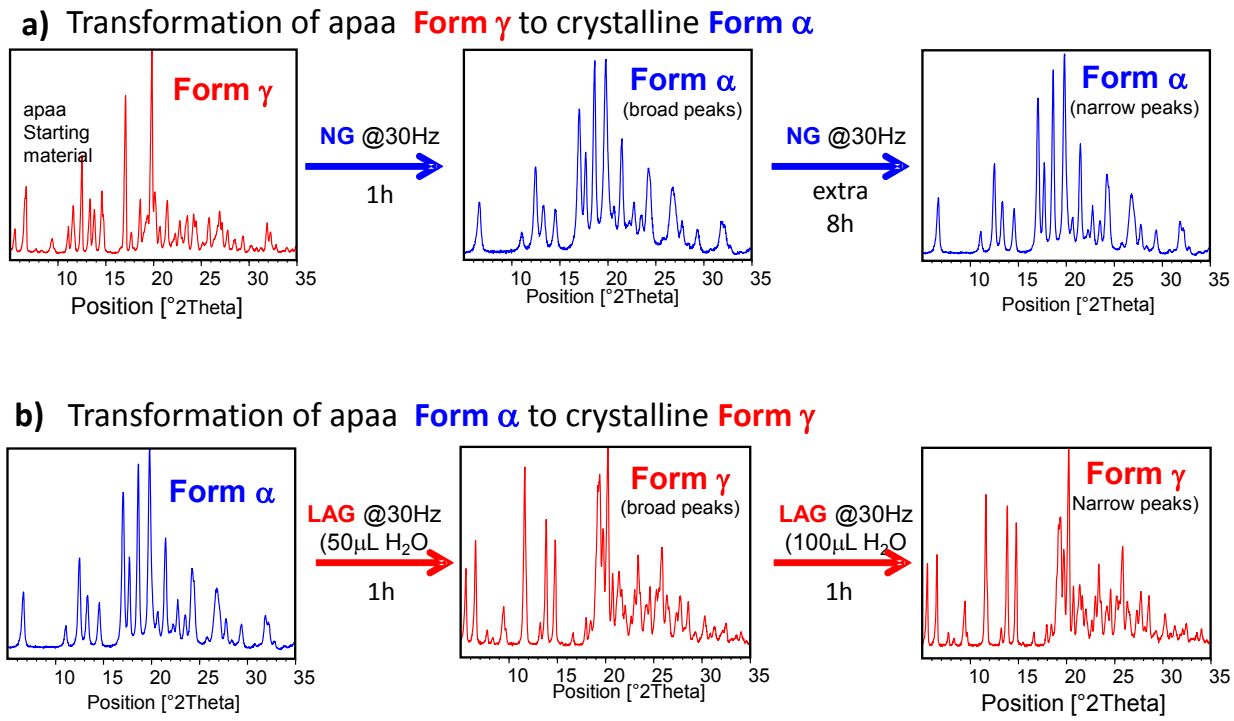

Figure S 16 Method development for the polymoprh transformation of the acetyl-L-phenylalanine amide (apaa) a) stable-bulk form γ to NG polymorph form α and b) form α to form γ by LAG. Extra grinding was performed in a) and b) to improve crystallinity of the material as shown by the narrower Braggs peaks.

4 *Experimental Section: Polymorph interconversion turnover experiments for single component system*

Polymorph interconversion turnover experiments for four single component systems: caffeine anhydrous, D-sorbitol, chlorpropamide and N-acetyl-L-phenylalanine amide.

4.1 Polymorph interconversion turnover experiments for Caffeine anhydrous

Starting from the commercially available anhydrous caffeine we have formed the NG-polymorph (NG-form) by NG and from this *in-situ* sample, the LAG polymorph (form II) by LAG using 50 μL MeCN. Two polymorph interconversion turnover cycles were performed.

Figure S 17a) shows the PXRD scans for set 1 while Figure S 17b) shows that for set 2. The superimposed PXRD traces for Set 1 is displayed on Figure 1 in the manuscript.

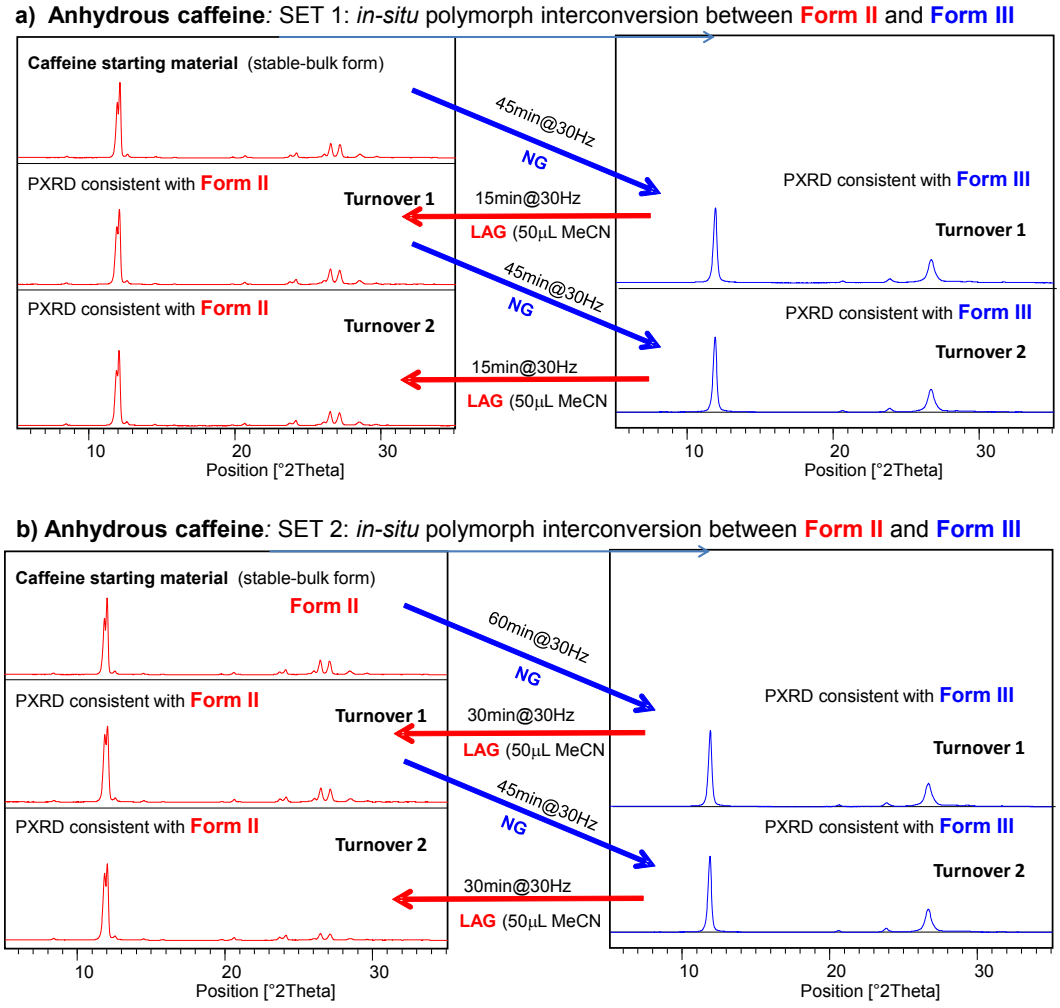

Figure S 17: Two set a) and b) each set has two cycles of polymorph interconversion turnover experiment starting from the commercially available product for caffeine anhydrous (form II). Tranformation of form II to NG-polymoprh form III by NG and back to form II by LAG. The experimental details and corresponding PXRDs are documented in the figure.

4.1.1 Determination of Scherrer crystalline size for caf

The size of the nanocrystals for anhydrous caffeine obtained from Set 1 of the polymorph interconversion turnover experiments and those performed to prepare sample for the SEM were estimated by Rietveld and Pawley refinements. They are tabulated in Table S2 and illustrated in Figure S18.

Table S 2 Conditions and outcome of turnover experiments and estimation of crystalline size for caf

Turnover experiments set 1: Ball mill reaction of Caffeine anhydrous (CAF) [58-0802]
(300 mg payload, 14.5 mL screw closure 440C stainless steel jar, 2x7.0 mm diameter 440C ss balls)

#	Turnover experiment	Starting material		Grinding conditions				PRODUCT Rietveld refinement*		PRODUCT Scherrer size				Quality of Refienement Data	
		Polymoprhic material to be milled	dried-in before next grinding	grinding time at 30Hz	solvent added to powder			Form III	Form II NIWFEE02	Form III		Form II NIWFEE03			
					LAG solvent type	solvent added µL	[solv/powder] (mmol/mol)	%M	%M	nm	esd %mol	nm	esd %mol	Rietveld refinement Goodness Rwp	Rietveld refinement Fit Index chisq
# 1	Turnover1--> stable---> metastable	Starting material	not dried	45 min	NG	0	0	100	0	55	0.5			9.1	3.2
# 2	Turnover1<-- metastable <--- stable	Form III	not dried	15 min	MeCN	50 uL	612	0	100			119	1.8	13.8	4.7
# 3	Turnover2--> stable---> metastable	Form II NIWFEE03	fumehood overnight	45 min	NG	0	0	100	0	52	0.6			10.6	3.6
# 4	Turnover2<-- metastable <--- stable	Form III	not dried	15 min	MeCN	50 uL	612	0	100			121	2.0	12.6	4.2
	fresh samples specific for the preparation of SEM sample														
# 5	SEM NG	Starting material	not dried	60 min	NG	0	0	100	0	55	0.5			9.1	3.2
# 6	SEM LAG	Form III	fumehood overnight	30 min	MeCN	50 uL	612	0	100			102	2.0	12.0	3.6

powder	MW	solvent	MW	density
caffeine	194.19	MeCN	41.05	0.7760

$$\mathrm{mmol_{MeCN}/mol_{CAF}} = \frac{\text{[illegible]} * \text{[illegible]} * \text{[illegible]}}{\text{[illegible]}}$$

e.s.d. = estimated standard deviation of the determination of crystal size from PXRD scans
Scherrer size estimated by Rietveld and Pawley refinements

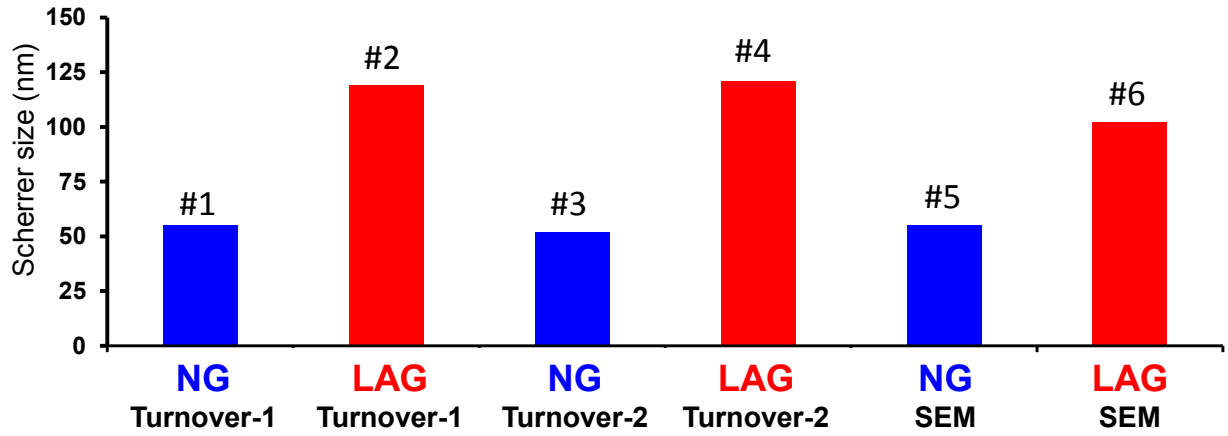

Figure S 18 Scherrer size for nanocrystals of anhydrous caffeine for the first set of turnover experiments obtained by NG and LAG, as estimated by Rietveld and Pawley refinements

4.1.2 SEM for NG- and LAG-polymorph of caf

These SEM images of anhydrous caffeine have been selected to show two secondary electron images for the NG-polymorph (Fig S 19 & S20 at 1μm and 500 nm bar scale) and for the LAG polymorph (Fig S 21 & S22 at 10μm and 2μm bar scale).

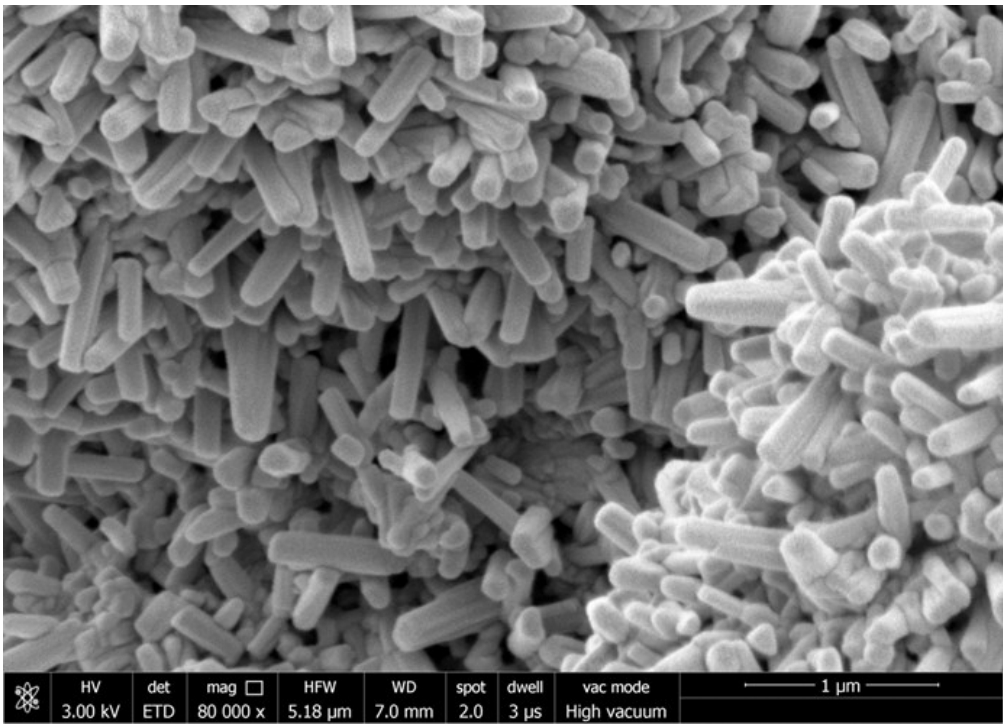

Figure S 19 Secondary electron image of a NG-polymorph (form III) milled powder sample of caf.

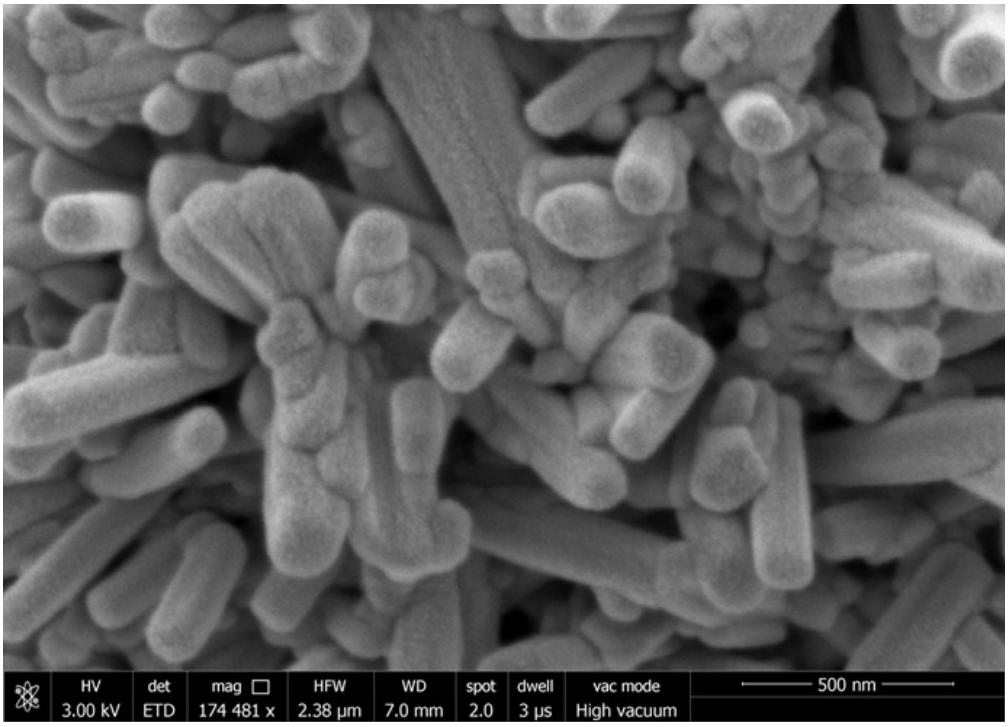

Figure S 20 Secondary electron image of a NG-polymorph (form III) milled powder sample of caf.

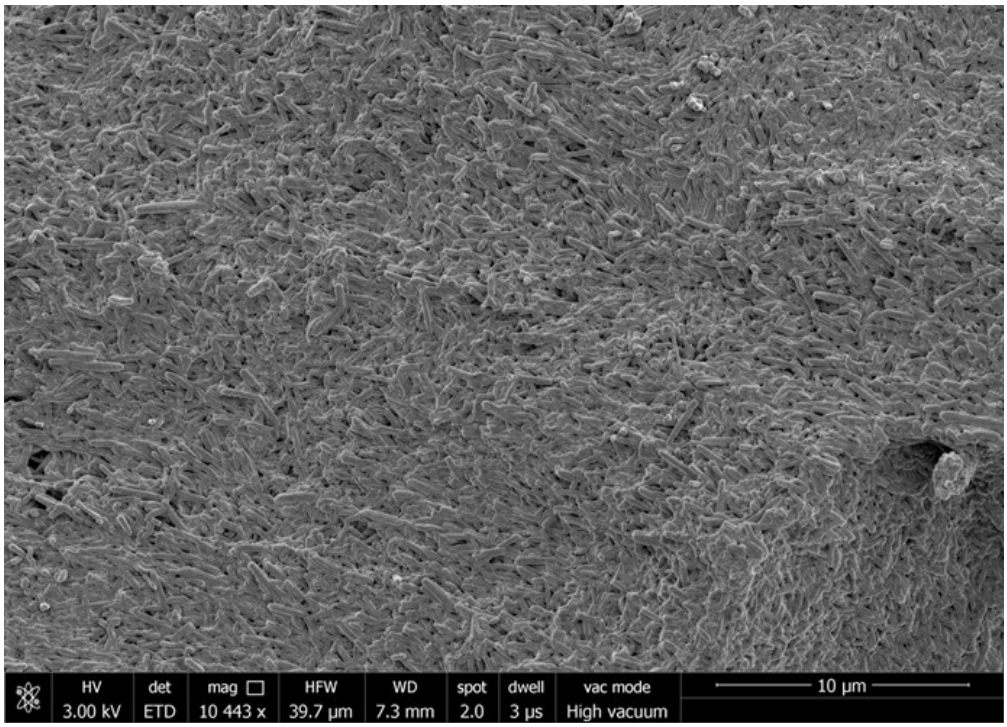

Figure S 21 Secondary electron image of a LAG-polymorph (form II) milled powder sample of caf

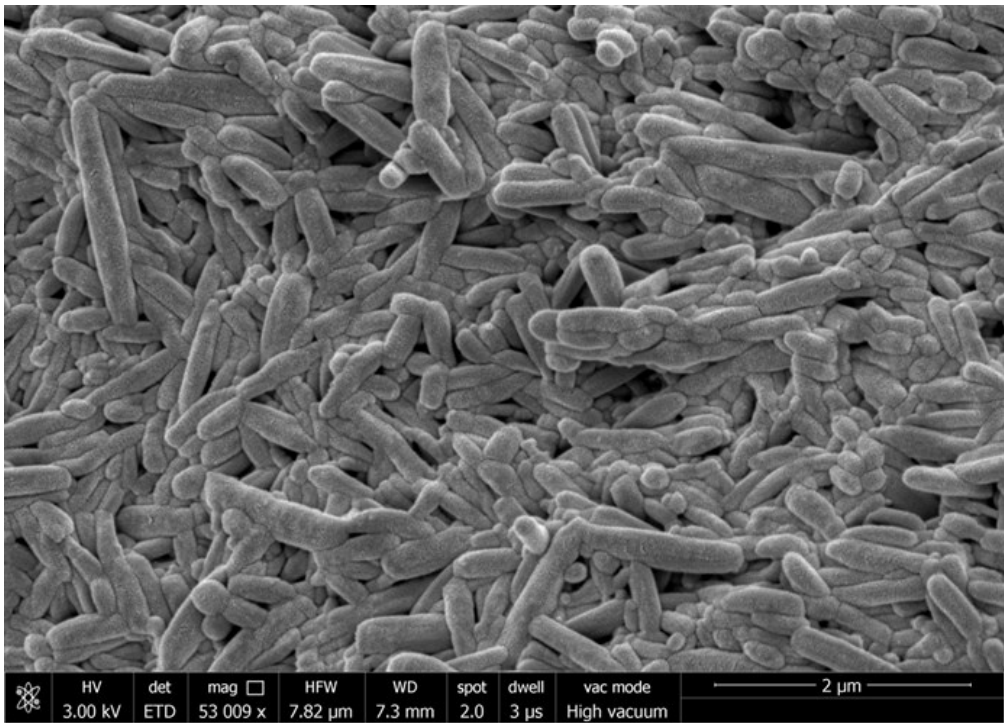

Figure S 22 Secondary electron image of a LAG-polymorph (form II) milled powder sample of caf.

4.2 Polymorph interconversion turnover experiments for D-Sorbitol

Starting from the commercially available D-sorbitol we have formed the NG polymorph by NG@30Hz and from this *in-situ* sample, the LAG polymorph by LAG @30Hz using 50 μL MeCN. Two polymorph interconversion turnover cycles were performed. Fig S23 shows the PXRD scans for each cycle. The superimposed PXRD traces is displayed on Figure 1 in the manuscript.

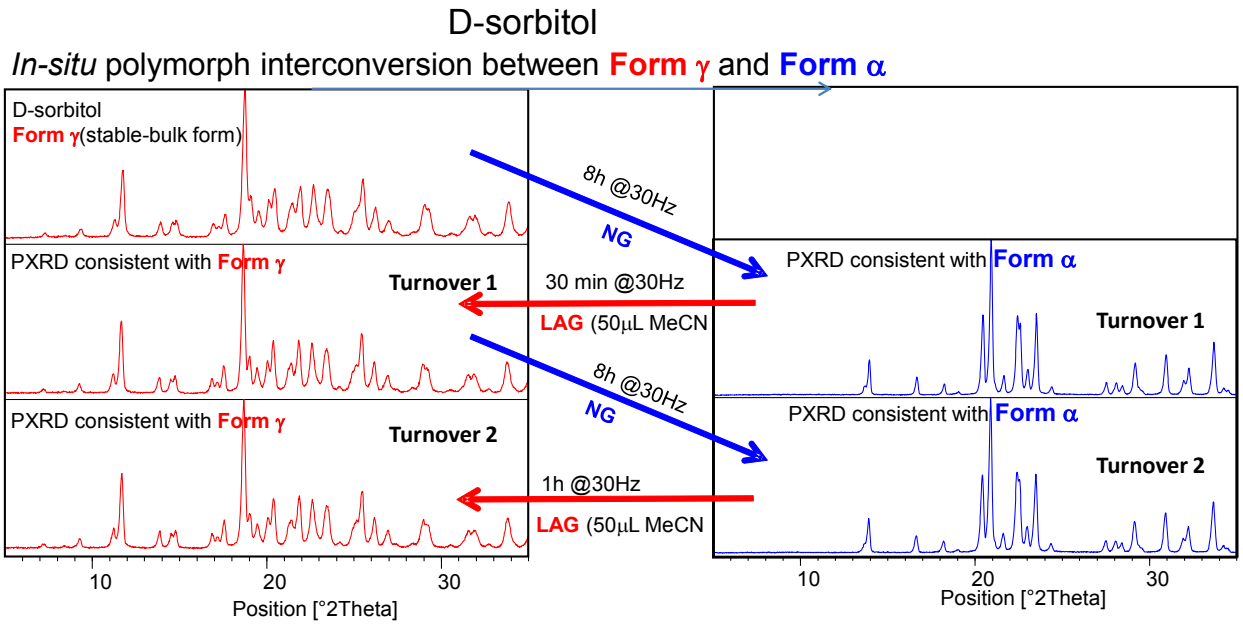

Figure S 23 Two cycles of polymorph interconversion turnover experiment starting from the commercially available product for D-sorbitol (stable-bulk polymorph, Form γ). Tranformation of Form γ to NG-polymoprh form α by NG and back to Form γ by LAG. The experimental details and corresponding PXRDs are documented in the figure.

4.2.1 Determination of Scherrer crystalline size

The size of the nanocrystals for D-sorbitol obtained from the polymorph interconversion turnover experiments and those performed to prepare sample for the SEM were estimated by Rietveld and Pawley refinements. They are tabulated in Table S3 and illustrated in Figure S24..

Table S 3 Conditions and outcome of turnover experiments and estimation of crystalline size for D-sor

Turnover experiments: Ball mill reaction of D-Sorbitol (D-Sor)

(300 mg payload, 14.5 mL screw closure 440C stainless steel jar, 2x7.0 mm diameter 440C ss balls)

#	Turnover experiment	Starting material		Grinding conditions				PRODUCT Rietveld refinement*		PRODUCT Scherrer size				Quality of Refienement Data	
		Polymoprhic material to be milled	dried-in before next grinding	grinding time at 30Hz	solvent added to powder			Form α GLUCIT01	Form γ GLUCIT03	Form α GLUCIT01		Form γ GLUCIT03			
					LAG solvent type	solvent added μL	[solv/powder] (mmol/mol)	%M	%M	nm	esd %mol	nm	esd %mol	Rietveld refinement Goodness Rwp	Rietveld refinement Fit Index chisq
# 1	Turnover1--> stable---> metastable	Starting material	not dried	8 h	NG	0	0	100	0	146	2.2			11.4	3.2
# 2	Turnover1<-- metastable <--- stable	Form α GLUCIT01	not dried	30 min	MeCN	50 uL	612	0	100			80	0.9	6.4	1.7
# 3	Turnover2--> stable---> metastable	Form γ GLUCIT03	desicator overnight	8 h	NG	0	0	100	0	118	1.8			10.6	2.7
# 4	Turnover2<-- metastable <--- stable	Form α GLUCIT01	not dried	1 h	MeCN	50 uL	612	0	100			75	0.8	6.8	1.9
fresh samples specific for the preparation of SEM sample															
# 3	SEM NG	Form γ GLUCIT03	desicator overnight	8 h	NG	0	0	100	0	118	1.8			10.6	2.7
# 6	SEM LAG	Form α GLUCIT01	not dried	1 h	MeCN	50 uL	612	0	100			117	1.5	7.6	2.0

powder	MW	solvent	MW	density
Sorbitol	194.19	MeCN	41.05	0.7760

$$mmol_{MeCN}/mol_{Sorbitol} = \frac{\text{[illegible]} * \text{[illegible]}}{\text{[illegible]}}$$

e.s.d. = estimated standard deviation of the determination of crystal size from PXRD scans ss = stainless steel

Scherrer size estimated by Rietveld and Pawley refinements

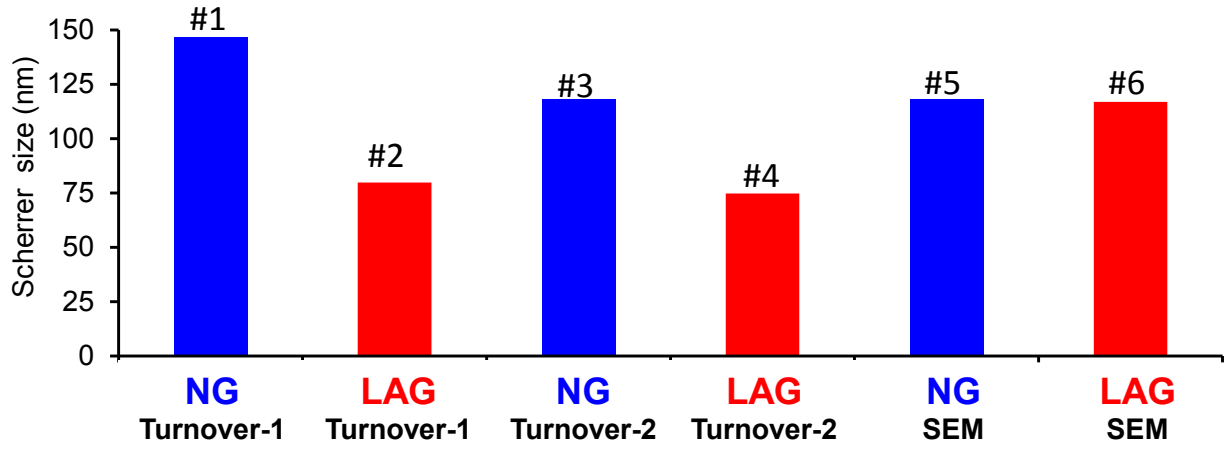

Figure S 24 Scherrer size for nanocrystals D-sorbitol for the first set of turnover experiments obtained by NG and LAG, as estimated by Rietveld and Pawley refinements

4.2.2 SEM for NG- and LAG-polymorph of D-sorbitol

These SEM images of D-sorbitol have been selected to show two secondary electron images for the NG-polymorph (Fig S 25 & S26 at 1μm and 1μm bar scale) and for the LAG polymorphs (Fig S 27 & S28 at 1μm and 1μm bar scale).

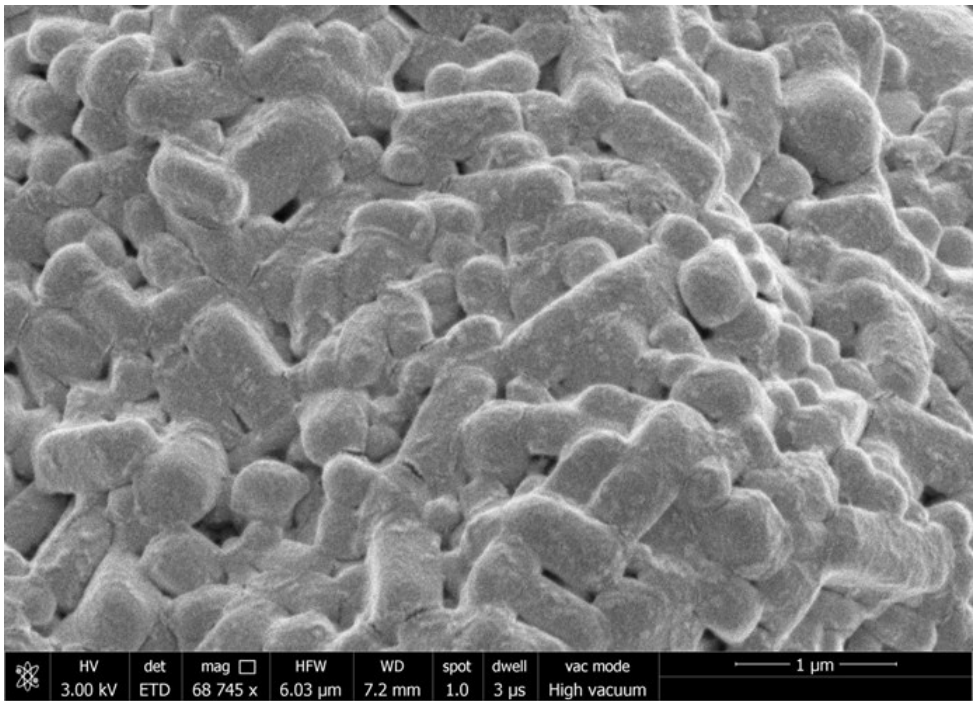

Figure S 25 Secondary electron image of a NG-polymorph (form α) milled powder sample of d-sor.

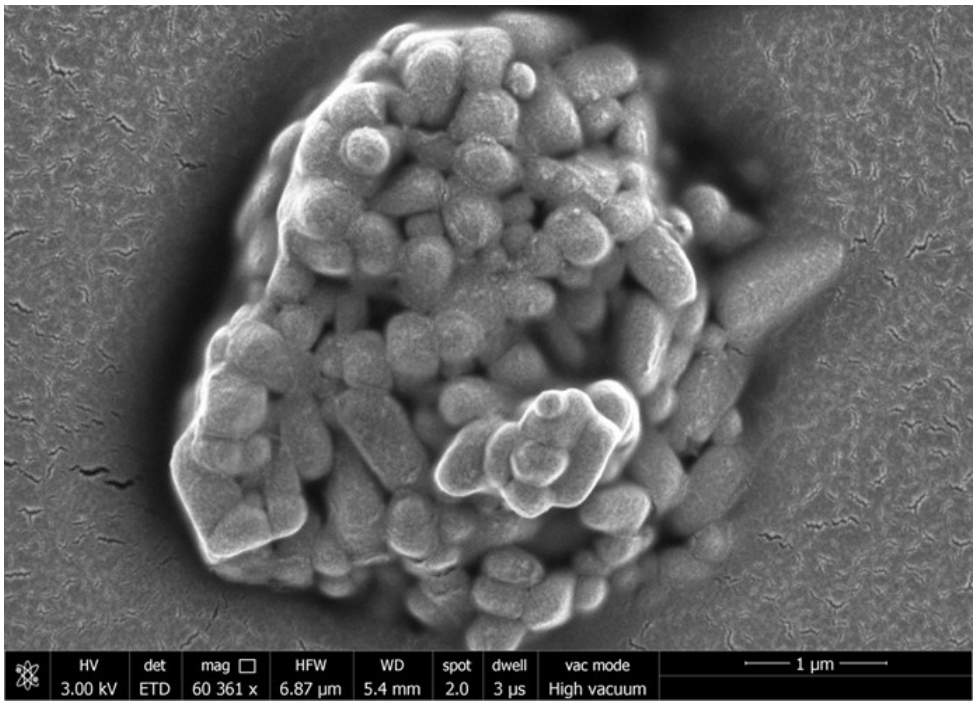

Figure S 26 Secondary electron image of a NG-polymorph (form α) milled powder sample of d-sor

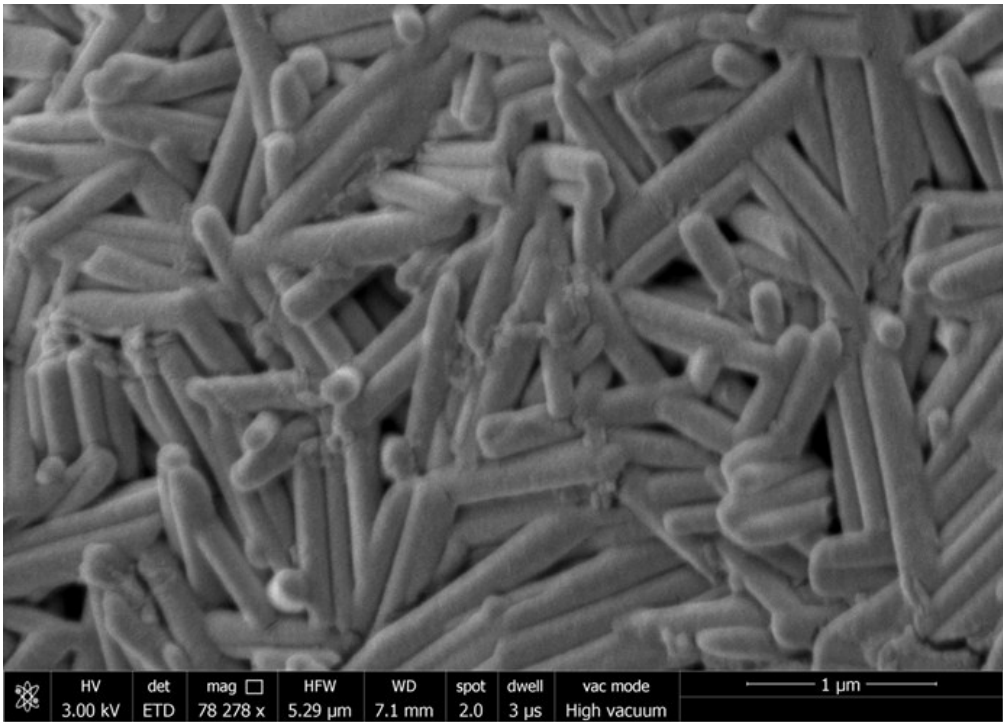

Figure S 27 Secondary electron image of a LAG-polymorph (Form γ) milled powder sample of d-sor

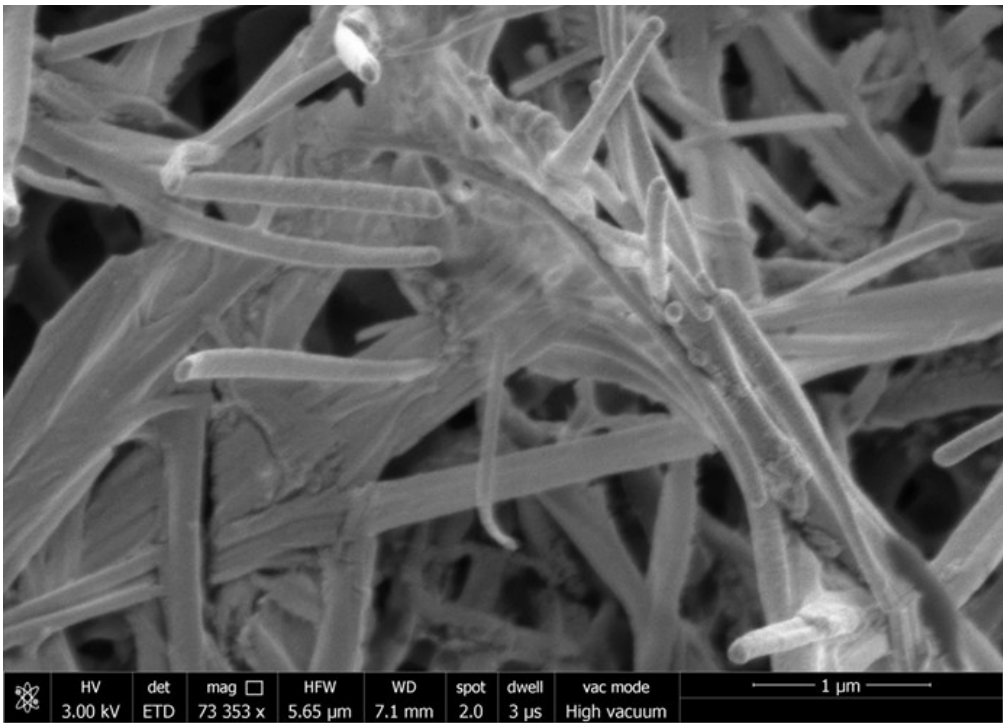

Figure S 28 Secondary electron image of a LAG-polymorph (Form γ) milled powder sample of d-sor

4.3 Polymorph interconversion turnover experiments for Chlorpropamide

Starting from the commercially available Chlorpropamide (form β) we have formed the NG polymorph (form η) by NG@30Hz and from this *in-situ* sample, the LAG polymorph (form β) by LAG @30Hz using 50 μL MeCN. Two polymorph interconversion turnover cycles were performed. Fig S17) shows the PXRD scans for each cycle. The superimposed PXRD traces is displayed on Figure 1 in manuscript.

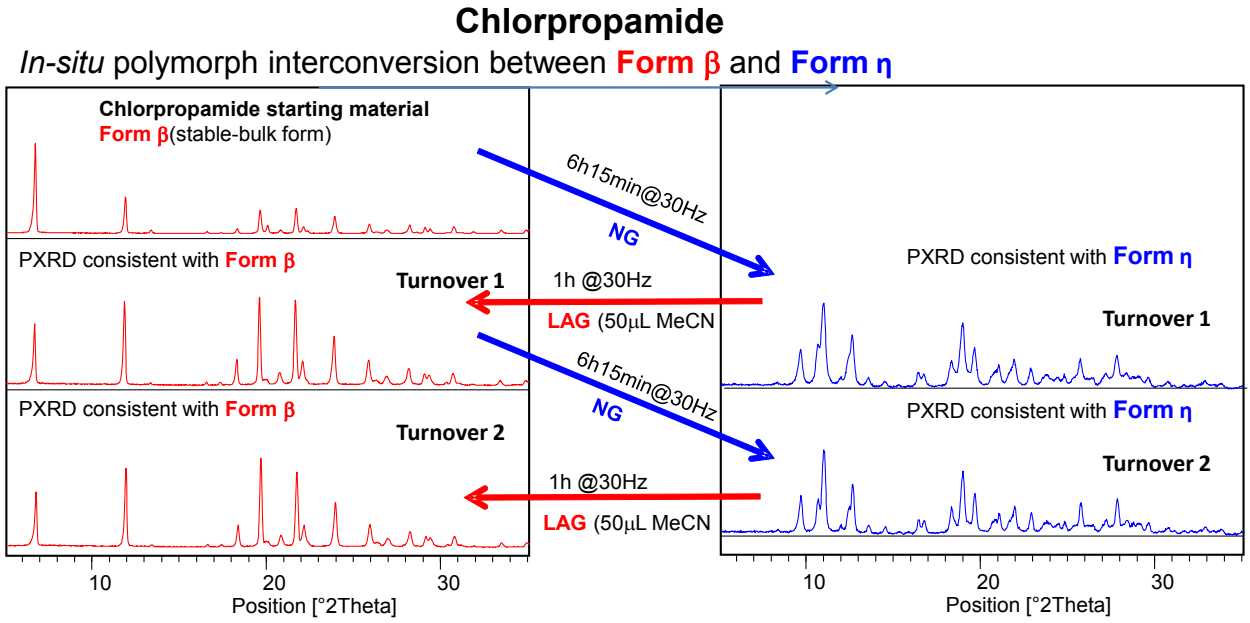

Figure S 29 Two cycles of polymorph interconversion turnover experiment starting from the commercially available material for chlorpropamide (stable-bulk polymorph, form β). Tranformation of form β to the metastable-bulk form η by NG and back to form β by LAG. The experimental details and corresponding PXRDs are documented in the figure.

4.3.1 Determination of Scherrer crystalline size for cpa

Table S 4 Conditions and outcome of turnover experiments and estimation of crystalline size for cpa

Turnover experiments: Ball mill reaction of Chlorpropamide (CPA) [94-20-2]

(300 mg payload, 14.5 mL screw closure 440C stainless steel jar, 2x7.0 mm diameter 440C ss balls)

#	Turnover experiment	Starting material		Grinding conditions				PRODUCT Rietveld refinement*		PRODUCT Scherrer size				Quality of Refienement Data	
					solvent added to powder			Form η	Form β	Form η		Form β			
		Polymoprhic material to be milled	dried-in before next grinding	grinding time at 30Hz	LAG solvent type	solvent added µL	[solv/powder] (mmol/mol)	%M	%M	nm	esd %mol	nm	esd %mol	Rietveld refinement Goodness **Rwp**	Rietveld refinement Fit Index **chisq**
# 1	**Turnover1-->** stable---> metastable	**Starting material**	not dried	**6h**	**NG**	**0**	**0**	**100** quantitative	**0** not present	**58**	0.9			5.4	1.2
# 2	**Turnover1<--** metastable <--- stable	**Form η**	not dried	**1 h**	**MeCN**	**50 uL**	**872**	**0.1**	**99.9**			**329**	13	13.6	2.7
# 3	**Turnover2-->** stable---> metastable	**Form β**	fumehood overnight	**8 h**	**NG**	**0**	**0**	**100** quantitative	**0** not present	**104**	2.0			5.4	1.2
# 4	**Turnover2<--** metastable <--- stable	**Form η**	not dried	**1 h**	**MeCN**	**50 uL**	**872**	**0.1**	**99.9**			**307**	11	14.4	2.9
	fresh samples specific for the preparation of SEM sample														
# 5	**SEM NG**	**Starting material**	not dried	**6h**	**NG**	**0**	**0**	**100** quantitative	**0** not present	**58**	1.0			5.6	1.3
# 6	**SEM LAG**	**Starting material**	not dried	**1 h**	**MeCN**	**50 uL**	**872**	**0.1**	**99.9**			**141**	4	11.6	2.1

powder	MW	solvent	MW	density
CPA	276.74	MeCN	41.05	0.7760

$$mmol_{MeCN} / mol_{Chlorpropamide} = \frac{\text{[illegible]} * \text{[illegible]} * \text{[illegible]}_{0.xxx} * \text{[illegible]}\ Chlorpropamide}{\text{[illegible]}\ Chlorpropamide_{x} * \text{[illegible]}_{0.xxx}}$$

e.s.d. = estimated standard deviation of the determination of crystal size from PXRD scans

Scherrer size estimated by Rietveld and Pawley refinements

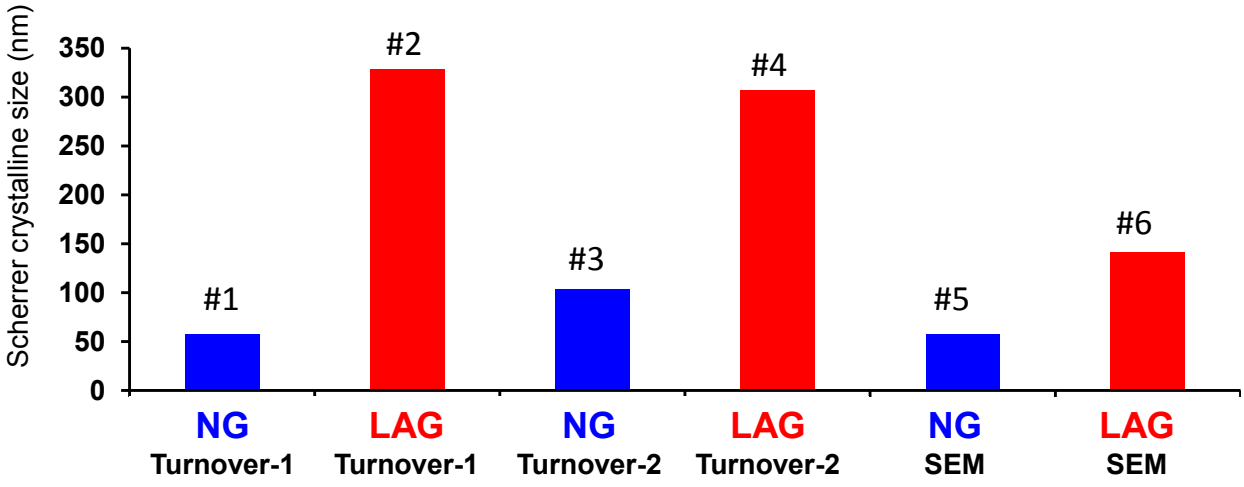

Figure S 30 Scherrer size for nanocrystals of chlorpropamide for the first set of turnover experiments obtained by NG and LAG, as estimated by Rietveld and Pawley refinements

4.3.2 SEM for NG-polymorph and LAG-polymorph of Chlorpropamide

These SEM images of chlorpropamide have been selected to show two secondary electron images for the NG-polymorph (Fig S 31 & S32 at 300nm and 300nm bar scale) and for the LAG polymorphs (Fig S 33 & S34 at 5μm and 5μm bar scale).

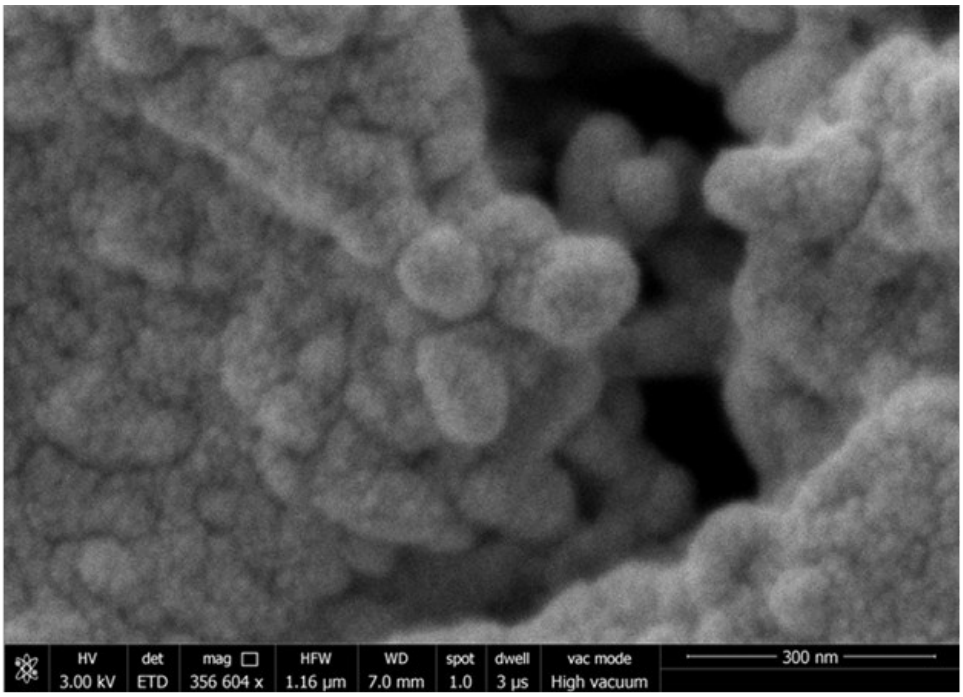

Figure S 31 Secondary electron image of a NG-polymorph (form η) milled powder sample of cpa.

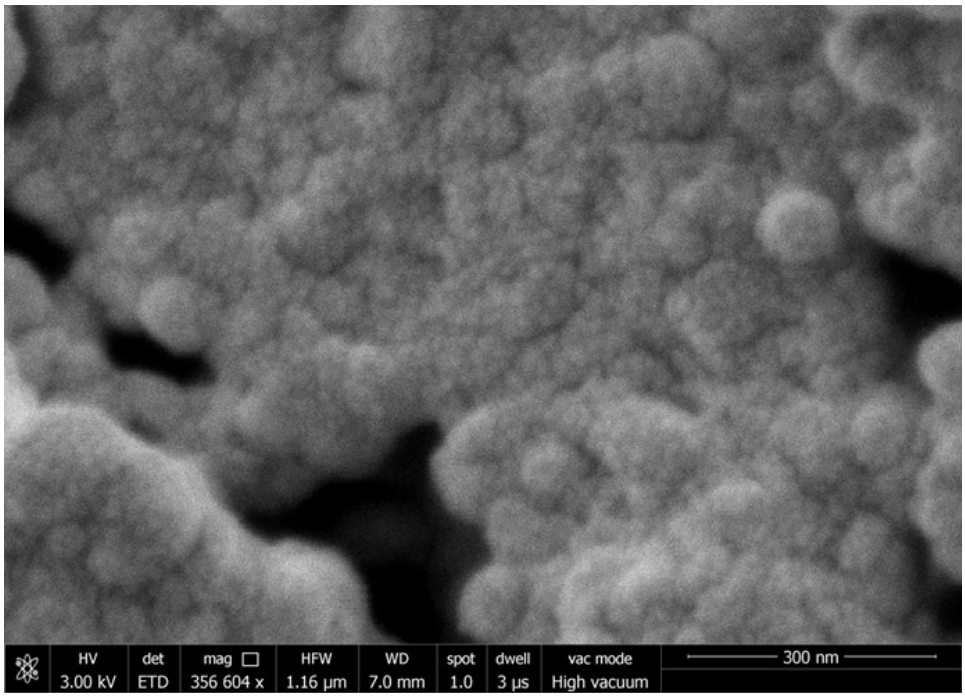

Figure S 32 Secondary electron image of a NG-polymorph (form η) milled powder sample of cpa.

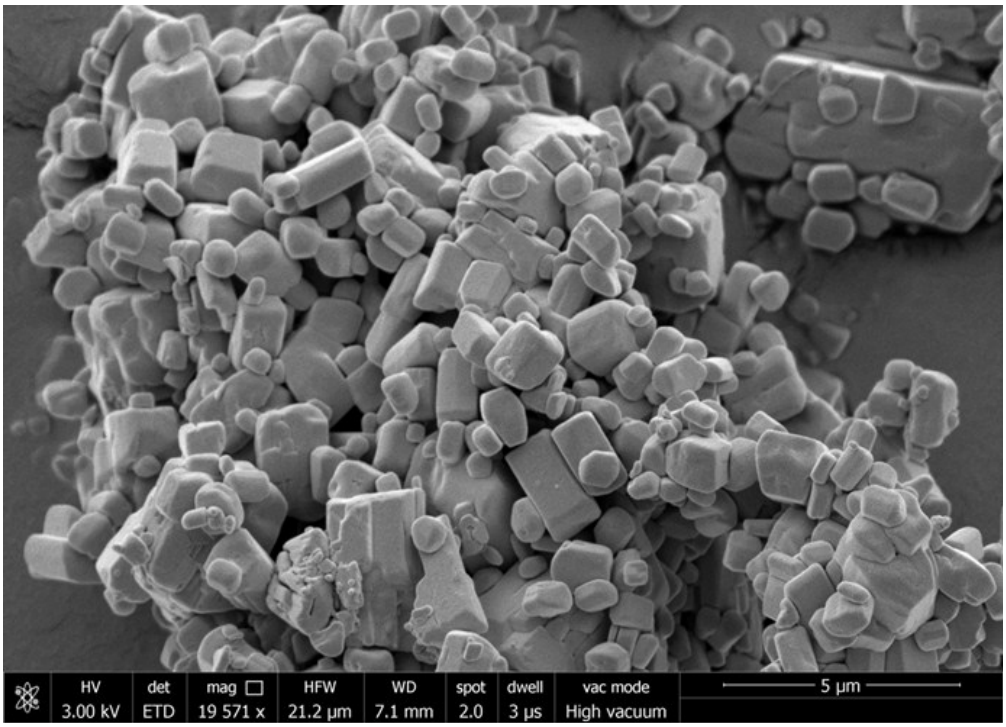

Figure S 33 Secondary electron image of a LAG-polymorph (form β) milled powder sample of cpa

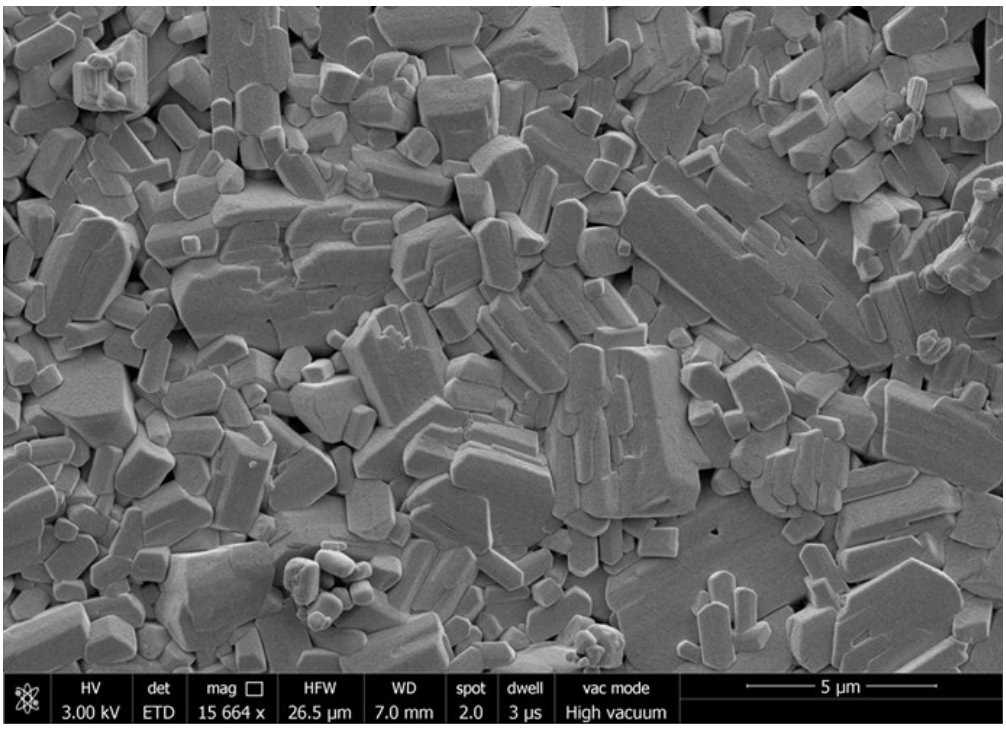

Figure S 34 Secondary electron image of a LAG-polymorph (form β) milled powder sample of cpa.

4.4 Polymorph interconversion turnover experiments for apaa

Starting from the commercially available N-acetyl-1-phenylalanine amide we have formed the NG polymorph by NG@30Hz and from this *in-situ* sample, the LAG polymorph by LAG @30Hz using 50 μL MeCN. Two polymorph interconversion turnover cycles were performed. Fig S35 shows the PXRD scans for each cycle. The superimposed PXRD traces is displayed on Figure 1 in manuscript.

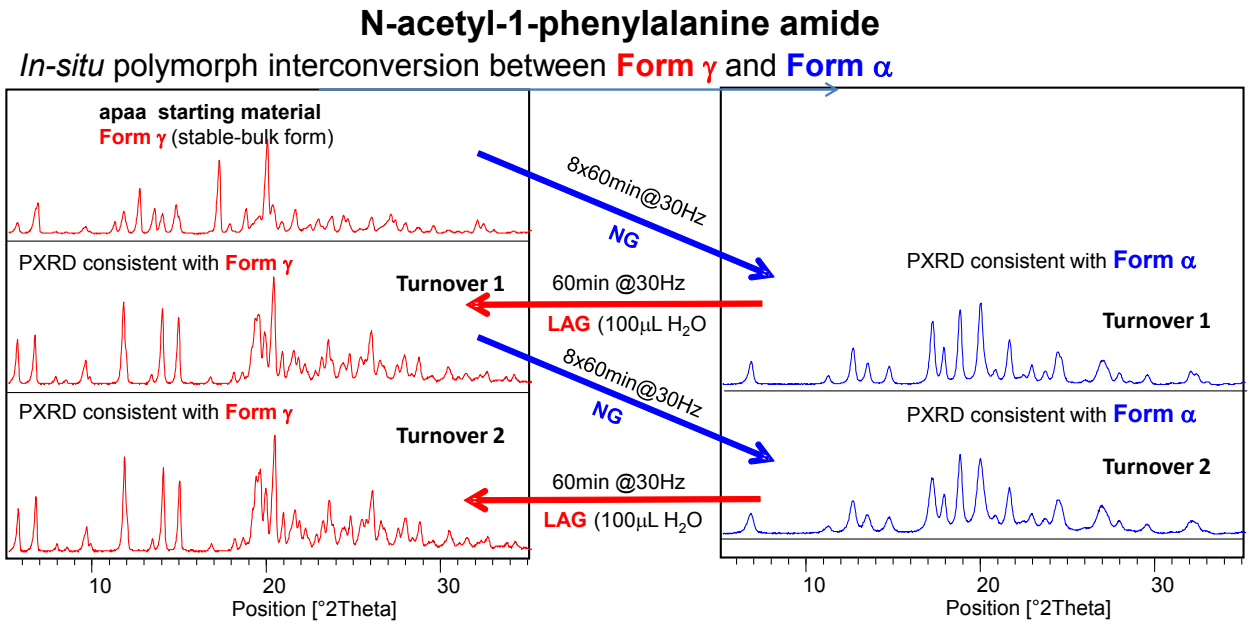

Figure S 35 Two cycles of polymorph interconversion turnover experiment starting from the commercially available product for N-acetyl-L-phenylalanine amide (stable-bulk polymorph, form γ). Tranformation of form γ to the NG-polymorph Form α by NG and back to form γ by LAG. The experimental details and corresponding PXRDs are documented in the figure.

4.4.1 Determination of Scherrer crystalline size for apaa

Table S 5 Conditions and outcome of turnover experiments and estimation of crystalline size for apaa

Turnover experiments: N-acetyl-1-phenylalanine amide (apaa) [7376-90-1]

(300 mg payload, 14.5 mL screw closure 440C stainless steel jar, 2x7.0 mm diameter 440C ss balls)

#	Turnover experiment	Starting material		Grinding conditions				PRODUCT Rietveld refinement*		PRODUCT Scherrer size				Quality of Refienement Data	
		Polymoprhic material to be milled	dried-in before next grinding	grinding time at 30Hz	solvent added to powder			Form α	Form γ	Form α		Form γ			
					LAG solvent type	solvent added µL	[solv/powder] (mmol/mol)	%M	%M	nm	esd %mol	nm	esd %mol	Rietveld refinement Goodness Rwp	Rietveld refinement Fit Index chisq
# 1	Turnover1--> stable---> metastable	Starting material	not dried	8h	NG	0	0	100	0	50	0.4			9.2	3.1
# 2	Turnover1<-- metastable <--- stable	Form α	not dried	1 h	water	100 uL	3809	0	100			137	3	9.3	2.8
# 3	Turnover2--> stable---> metastable	Form γ	fumehood overnight	8 h	NG	0	0	100	0	31	0.3			7.8	2.5
# 4	Turnover2<-- metastable <--- stable	Form α	not dried	1 h	water	100 uL	3809	0	100			157	4	8.0	2.6
	fresh samples specific for the preparation of SEM sample														
# 5	SEM NG	Form γ	overnight fumehood	1 h	NG	0		100.0	0.0	26	0.3			7.7	2.4
# 6	SEM LAG	Form α	not dried	1 h	water	100 uL	3809	0	100			150			

powder	MW	solvent	MW	density
apaa	206.24	water	18.00	0.9974

$$mmol_{H_2O}\ /mol_{apaa} = \frac{\text{[illegible]} * \text{[illegible]}_{g\ mmol} * \text{[illegible]}_{g\ mmol} * \text{[illegible]}_{apaa}}{\text{[illegible]}_{apaa} * \text{[illegible]}_{g\ mmol}}$$

e.s.d. = estimated standard deviation of the determination of crystal size from PXRD scans

ss = stainless steel

Scherrer size estimated by Rietveld and Pawley refinements

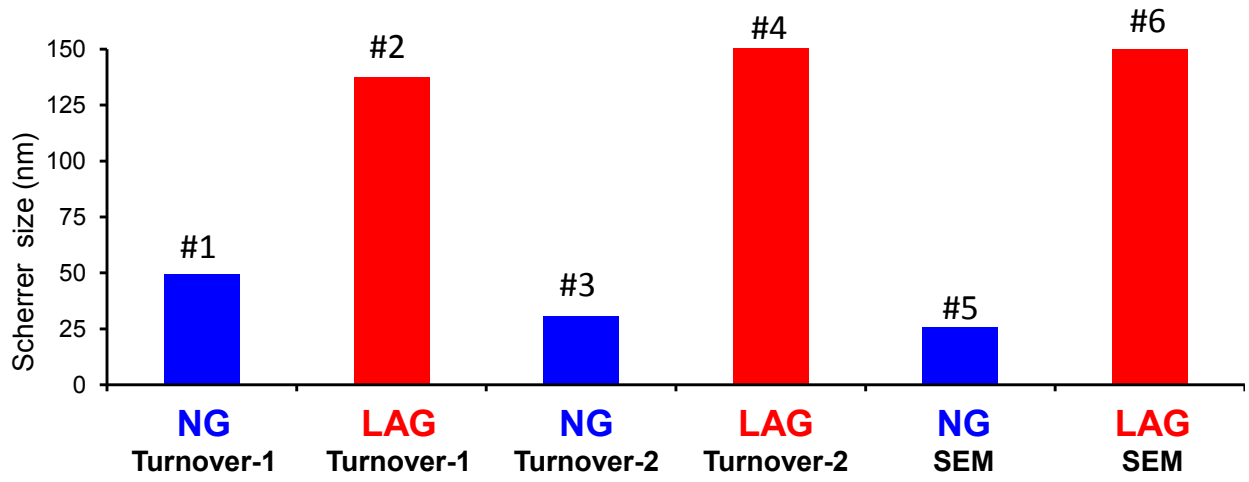

Figure S 36 Scherrer size for nanocrystals of N-acetyl-1-phenylalanine amide for the first set of turnover experiments obtained by NG and LAG, as estimated by Rietveld and Pawley refinements

4.4.2 SEM for NG-polymorph and LAG-polymorph of for APAA

These SEM images of N-acetyl-L-phenylalanine amide have been selected to show two secondary electron images for the NG-polymorph (Fig S 37 & S38 at 2μm and 500nm bar scale) and for the LAG polymorphs (Fig S 39 & S40 at 5μm and 1μm bar scale).

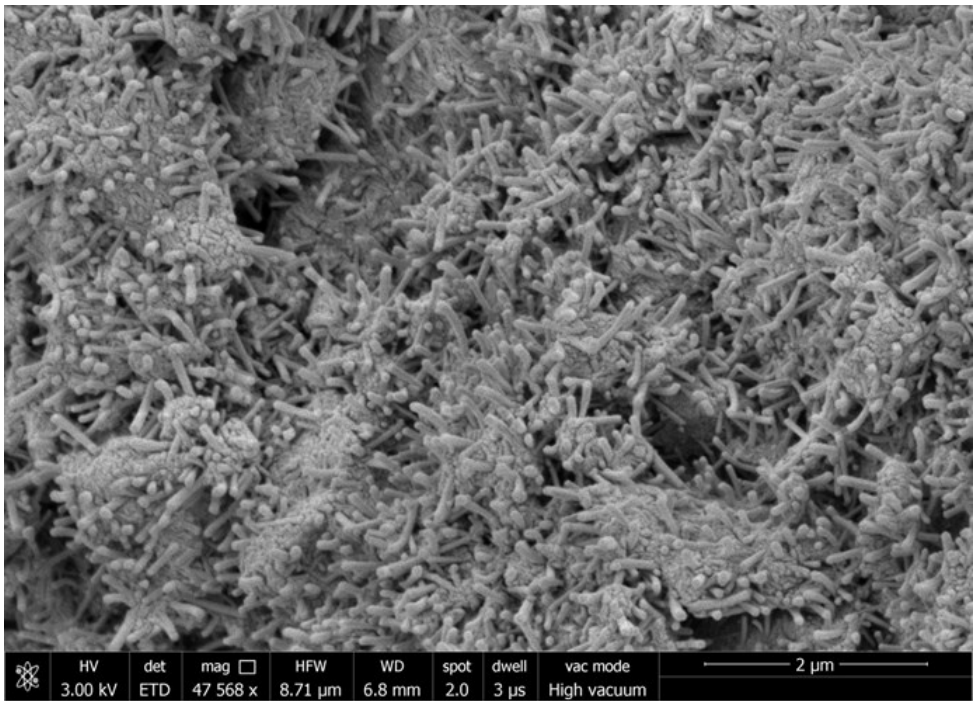

Figure S 37 Secondary electron image of a NG-polymorph (form α) milled powder sample of apaa

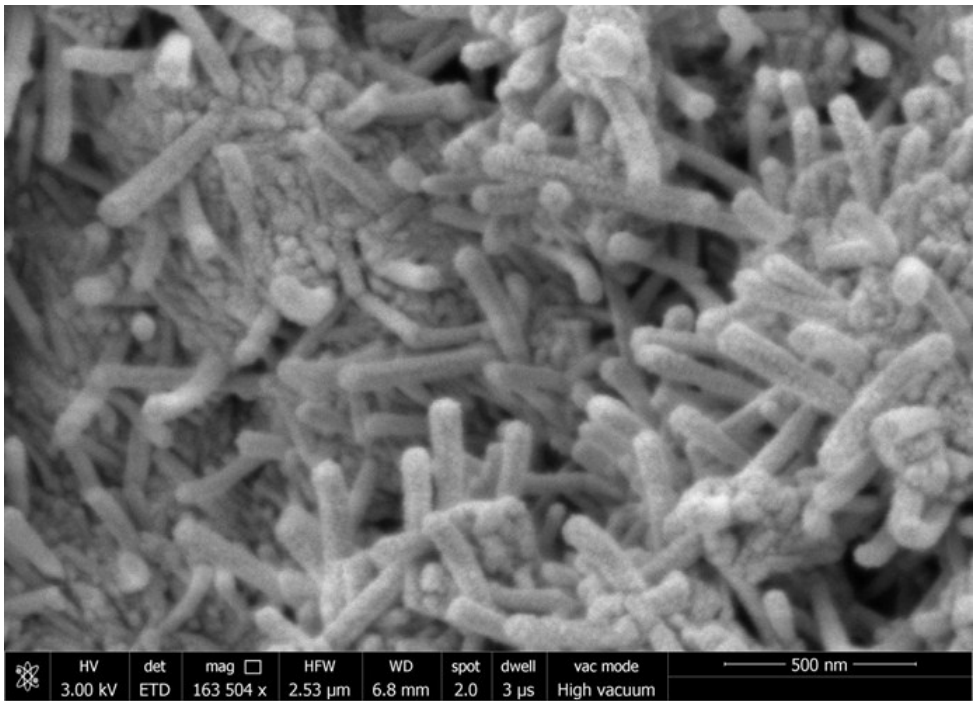

Figure S 38 Secondary electron image of a NG-polymorph (form α) milled powder sample of apaa.

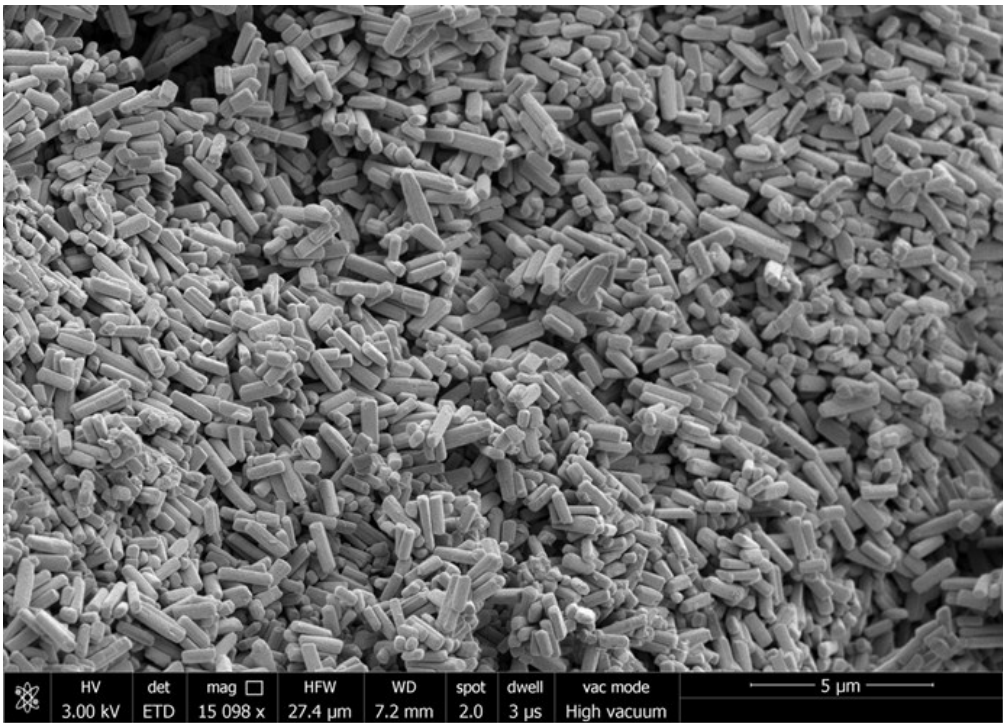

Figure S 39 Secondary electron image of a LAG-polymorph (form γ) milled powder sample of apaa.

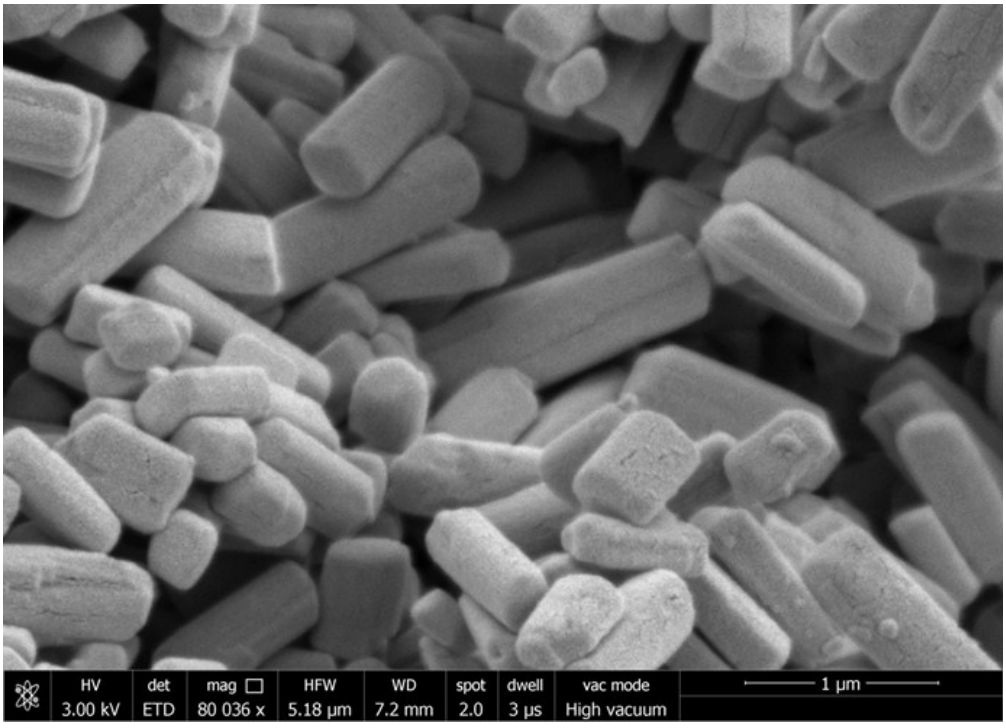

Figure S 40 Secondary electron image of a LAG-polymorph (form γ) milled powder sample of apaa.

5 References

1. Belenguer, A. M.; Friscic, T.; Day, G. M.; Sanders, J. K. M., Solid-state dynamic combinatorial chemistry: reversibility and thermodynamic product selection in covalent mechanosynthesis. *Chem. Sci.* 2011, *2* (4), 696.

2. Belenguer, A. M.; Lampronti, G. I.; Wales, D. J.; Sanders, J. K. M., Direct Observation of Intermediates in a Thermodynamically Controlled Solid-State Dynamic Covalent Reaction. *J. Am. Chem. Soc.* 2014, *136* (46), 16156.

3. Willart, J.-F.; Lefebvre, J.; Danède, F.; Comini, S.; Looten, P.; Descamps, M., Polymorphic transformation of the Γ-form of d-sorbitol upon milling: structural and nanostructural analyses. *Solid State Communications* 2005, *135* (8), 519.

4. Belenguer, A. M.; Lampronti, G. I.; Sanders, J. K. M., Reliable Mechanochemistry: Protocols for Reproducible Outcomes of Neat and Liquid Assisted Ball-mill Grinding Experiments. *JoVE* 2018, (131), e56824.

5. Belenguer, A. M.; Lampronti, G. I.; Cruz-Cabeza, A. J.; Hunter, C. A.; Sanders, J. K. M., Solvation and surface effects on polymorph stabilities at the nanoscale. *Chem. Sci.* 2016, *7* (11), 6617.

6. Altheimer, B. D.; Pagola, S.; Zeller, M.; Mehta, M. A., Mechanochemical Conversions Between Crystalline Polymorphs of a Complex Organic Solid. *Cryst. Growth Des.* 2013, *13* (8), 3447.

7. Coelho, A. A., TOPAS and TOPAS-Academic: an optimization program integrating computer algebra and crystallographic objects written in C++. *Journal of Applied Crystallography* 2018, *51* (1), 210.

8. Allen, F., The Cambridge Structural Database: a quarter of a million crystal structures and rising. *Acta Crystallographica Section B* 2002, *58* (3 Part 1), 380.

9. Payzant, E. A., *"Other Topics" in Principles and Applications of Powder Diffraction edited by Clearfield, A, Reibenspies, J. H. and Bhuvanesh N.* John Wiley and Sons, Ltd: 2008; p 365.

10. Michalchuk, A. A. L.; Tumanov, I. A.; Boldyreva, E. V., The effect of ball mass on the mechanochemical transformation of a single-component organic system: anhydrous caffeine. *Journal of Materials Science* 2018, *53* (19), 13380.

11. Hédoux, A.; Guinet, Y.; Paccou, L.; Danède, F.; Derollez, P., Polymorphic transformation of anhydrous caffeine upon grinding and hydrostatic pressurizing analyzed by low-frequency raman spectroscopy. *Journal of Pharmaceutical Sciences* 2013, *102* (1), 162.

12. Drebushchak, T. N.; Ogienko, A. A.; Boldyreva, E. V., 'Hedvall effect' in cryogrinding of molecular crystals. A case study of a polymorphic transition in chlorpropamide. *CrystEngComm* 2011, *13* (13), 4405.

13. Bouvart, N.; Palix, R.-M.; Arkhipov, S. G.; Tumanov, I. A.; Michalchuk, A. A. L.; Boldyreva, E. V., Polymorphism of chlorpropamide on liquid-assisted mechanical treatment: choice of liquid and type of mechanical treatment matter. *CrystEngComm* 2018.